AD-A152 763 A NUMERICAL STUDY OF THE MEAN TRAJECTORY APPROXIMATION IN A NON-ADIABATIC PROCESS(U) CALIFORNIA UNIV SANTA BARBARA DEPT OF CHEMISTRY S SAWADA ET AL. MAR 85 TR-18 1/1

UNCLASSIFIED N00014-81-K-0598 F/G 20/8 NL

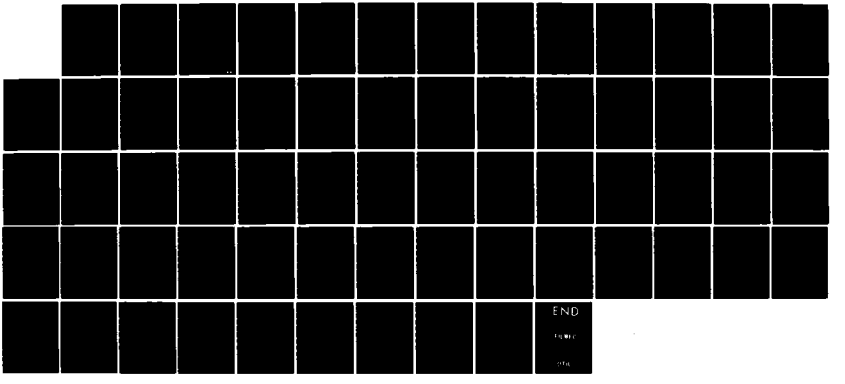

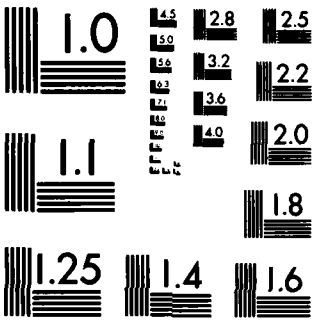

MICROCOPY RESOLUTION TEST CHART
NATIONAL BUREAU OF STANDARDS-1963-A

unclassified/unlimited
SECURITY CLASSIFICATION OF THIS PAGE (When Data Entered)

(2)

REPORT DOCUMENTATION PAGE

READ INSTRUCTIONS BEFORE COMPLETING FORM

1. REPORT NUMBER: 18
2. GOVT ACCESSION NO.:
3. RECIPIENT'S CATALOG NUMBER:

4. TITLE (and Subtitle): A NUMERICAL STUDY OF THE MEAN TRAJECTORY APPROXIMATION IN A NON-ADIABATIC PROCESS
5. TYPE OF REPORT & PERIOD COVERED: Annual Technical Report
6. PERFORMING ORG. REPORT NUMBER:

7. AUTHOR(s): Shin-ichi Sawada and Horia Metiu
8. CONTRACT OR GRANT NUMBER(s): N00014-81-K-0598

9. PERFORMING ORGANIZATION NAME AND ADDRESS:
University of California
Department of Chemistry
Santa Barbara, Ca. 93106

10. PROGRAM ELEMENT, PROJECT, TASK AREA & WORK UNIT NUMBERS: NR 056-766/4-21-81 (472)

11. CONTROLLING OFFICE NAME AND ADDRESS:
Office of Naval Research
Department of the Navy, Code: 612A: DKB
Arlington, VA 22217

12. REPORT DATE: March 1985
13. NUMBER OF PAGES: 58

14. MONITORING AGENCY NAME & ADDRESS (if different from Controlling Office):
Office of Naval Research Detachment Pasadena
1030 East Green Street
Pasadena, CA 91105

15. SECURITY CLASS. (of this report): unclassified/unlimited
15a. DECLASSIFICATION/DOWNGRADING SCHEDULE:

16. DISTRIBUTION STATEMENT (of this Report)

This document has been approved for public release and sale; its distribution is unlimited.

17. DISTRIBUTION STATEMENT (of the abstract entered in Block 20, if different from Report)

This document has been approved for public release and sale; its distribution is unlimited.

18. SUPPLEMENTARY NOTES

Submitted to Phys. Rev. B

19. KEY WORDS (Continue on reverse side if necessary and identify by block number)

20. ABSTRACT (Continue on reverse side if necessary and identify by block number)

We present numerical results obtained with the mean trajectory approximation applied to a non-adiabatic process described by a curve crossing model. We compare them to the results given by the customary trajectory approximation which uses one adiabatic potential to generate the nuclear motion, and to the results given by Nikitin's formula. We find that at low kinetic energy the three procedures give very different results. The differences are caused by the fact that the mean trajectory method includes quantum effects in the effective potential used for the classical motion. We also discover an unex-

DD FORM 1 JAN 73 1473 EDITION OF 1 NOV 65 IS OBSOLETE
S/N 0102-LF-014-6601

unclassified/unlimited
SECURITY CLASSIFICATION OF THIS PAGE (When Data Entered)

pected behavior: under certain conditions the transition probability seems to become a random function of the incident energy.

OFFICE OF NAVAL RESEARCH

Contract N00014-81-K-0598

Task No. NR 056-766/4-21-81 (472)

Technical Report No. 18

A NUMERICAL STUDY THE MEAN TRAJECTORY APPROXIMATION IN A NON-ADIABATIC PROCESS

by

S. Sawada and H. Metiu

PHYS. REV. B, submitted (1985)

University of California
Department of Chemistry
Santa Barbara, CA 93106

A NUMERICAL STUDY OF THE MEAN TRAJECTORY APPROXIMATION IN A NON-ADIABATIC PROCESS

Shin-ichi Sawada and Horia Metiu

Department of Chemistry
University of California
Santa Barbara, California 93106

ABSTRACT

We present numerical results obtained with the mean trajectory approximation applied to a non-adiabatic process described by a curve crossing model. We compare them to the results given by the customary trajectory approximation which uses one adiabatic potential to generate the nuclear motion, and to the results given by Nikitin's formula. We find that at low kinetic energy the three procedures give very different results. The differences are caused by the fact that the mean trajectory method includes quantum effects in the effective potential used for the classical motion. We also discover an unexpected behavior: under certain conditions the transition probability seems to become a random function of the incident energy.

I. INTRODUCTION

The description of the dynamics of a large number of surface science phenomena requires non-adiabatic models in which the system undergoes transitions between at least two states. It is customary to treat such problems by using quantum theory for the non-adiabatic states and classical equations for the other degrees of freedom.[1] If the energy of the classical variables is low compared to the energy difference between the states, this method becomes ambiguous and inadequate. In a previous paper we reviewed and explained this situation and proposed a better, but still inexact, method which we call the mean trajectory approximation.[2] In this article we present a detailed numerical study of this method.

The application is made to a model problem in which a particle approaches a surface and undergoes a transition from one electronic state to another. Since the particle is heavy we intend to treat its nuclear motion by a classical method. However, since in the interaction region the electronic state of the particle is a coherent superposition of the two electronic states mentioned above, we do not have a unique prescription for writing the force acting on the particle in the classical equation of motion. By using systematic methods to take the classical limit for the nuclear motion MTA arrives at a prescription in which the "classical" potential is a certain quantum mean of the electronic matrix elements. This is a time dependent potential which varies as the collision changes the occupation of the two states. If the state i is highly occupied throughout the collision the effective potential resembles the potential energy curve $H_{ii}(R)$ of that state. If the occupation changes from 1 to 2 the effective potential switches its character from resembling $H_{11}(R)$ to resembling $H_{22}(R)$. Of course intermediate situations in which the potential is an evenly weighted combination of H_{11} and H_{22} are also possible.

The present paper explores numerically the properties of the effective potential, of the resulting nuclear trajectory and the differences between MTA and the usual trajectory approximation (TA). One of the more striking results of such calculations occurs when the coupling between the diabatic states is small and the kinetic energy is low. Under these conditions the mean potential can become larger than the classical total energy of the particle and temporarily trap the particle at the surface. When this happens the asymptotic value of the probabilty of emerging on a specified state seems to become a discontinuous, random function of the kinetic energy.

II. NUMERICAL RESULTS FOR TWO STATES CROSSING

II.1 Summary of the Equations

Since the theory was presented in a previous article[2] we give here only the equations used in the numerical calculations, to the extent needed to clarify the notation. We use the wave function

$$\psi(R,x;t) = c_1(t)\ \Phi_1(x,R(t)) + c_2(t)\ \Phi_2(x,R(t)) \qquad (2.1)$$

where x represents the coordinates of the electrons, R(t) are the positions of the nuclei at time t, Φ_i, i = 1,2 are electronic diabatic states and $c_i(t)$ are complex probability amplitudes. The ortho-normality relation

$$\int \Phi^*_\alpha (x,R(t))\ \Phi_\beta(x,R(t))\ dx = \delta_{\alpha\beta} \qquad (2.2)$$

is assumed throughout. The amplitudes $c_i(t)$ satisfy the equations

$$i\hbar\dot{c}_\alpha = H_{\alpha\alpha}(R(t))\ c_\alpha(t) + H_{\alpha\beta}(R(t))\ c_\beta(t) \qquad (2.3)$$

with α = 1 or 2, β = 1 or 2 and $\beta \neq \alpha$, and $\dot{c}_\alpha = dc_\alpha/dt$.

For the matrix elements $H_{\alpha\beta}(R(t))$ we chose

$$H_{11}(R(t)) = U_o((R_o/R)\ \exp[-2(R-R_o)]\ -2\exp[-(R-R_o)]) + \lambda/2 \qquad (2.4a)$$

$$H_{22}(R(t)) = U_o((R_o/R)\ \exp[-2(R-R_o)] + 2\exp[-(R-R_o)]) - \lambda/2 \qquad (2.4b)$$

and

$$H_{12}(R(t)) = H_{21}(R(t)) = -2\beta U_o \exp[-(R-R_o)] \quad . \qquad (2.4c)$$

The functions $H_{11}(R)$ and $H_{22}(R)$ are the diabatic energy curves of the two states $\Phi_\alpha(x,R(t))$. They are plotted in Fig. 1 as full lines. The curve H_{11} is a Morse potential (which we multiplied by (R_o/R), to make the repulsive energy infinite at short surface particle distances R) to which we added a constant energy $\Delta\epsilon/2$. The curve H_{22} is modified to have smaller binding energy than H_{11}. The coupling H_{12} dies off exponentially on the same length scale as the potentials and becomes constant at short distances. The coupling constant is β.

The equations (2.3) and (2.4) are written in terms of dimensionless variables. The length unit α^{-1} is given by the inverse length α appearing in the Morse potential $V(y) = U_o(\exp[-2\alpha(y-y_o)] - \exp(-\alpha(y-y_o)))$. The length α^{-1} is the range of the potentials H_{11} and H_{22}. The time unit is $(\alpha v_o)^{-1}$, where v_o is the velocity of the incident particle. For energy we use $\hbar\alpha v_o$ and for mass $(\hbar\alpha/v_o)$. An important dimensionless quantity is the Massey parameter

$$\lambda = \Delta\epsilon/\hbar\alpha v_o \quad , \qquad (2.5)$$

where $\Delta\epsilon$ is the asymptotic energy gap between the states (i.e. $\Delta\epsilon = \lim(H_{11}(R) - H_{22}(R))$ for $R \to \infty$). The values of the parameters used in the present calculations are given in Table I.

We find it useful sometimes to switch between the diabatic and the adiabatic pictures. Therefore we present briefly the equations used to make this connection. Since the time dependence appears through R only we can write the Eqs. (2.3) (using an obvious, two dimensional matrix notation) as

$$(i\hbar v)\, \partial\vec{c}/\partial R = \overleftrightarrow{H} \cdot \vec{c} \qquad (2.6)$$

with $v \equiv \dot{R}$. Since we have assumed that the diabatic states are

orthonormal we can use an unitary matrix

$$\overleftrightarrow{U} \equiv \begin{pmatrix} \cos\theta & ; & \sin\theta \\ -\sin\theta & ; & \cos\theta \end{pmatrix} \tag{2.7}$$

with

$$\tan 2\theta = 2H_{12}(H_{22}-H_{11})^{-1} \quad . \tag{2.8}$$

The adiabatic surfaces are given by

$$H^a_{\alpha\alpha}(R) = (U^{-1})_{\alpha\gamma} H_{\gamma\mu} U_{\mu\alpha} \quad , \ \alpha = 1 \text{ or } 2, \tag{2.9}$$

(repeated indeces are summed over) and the adiabatic amplitudes by

$$c^a_\alpha = (U^{-1})_{\alpha\mu} c_\mu \qquad \alpha = 1 \text{ or } 2 \quad . \tag{2.10}$$

Defining

$$c^a_\alpha \equiv \tilde{c}_\alpha \exp\{(i/\hbar) \int_\infty^R (H^a_{\alpha\alpha}(R)/\dot{R})dR\} \tag{2.11}$$

and using the above equations in (Eq.2.3) leads to

$$\partial\tilde{c}_\alpha/\partial R = (-1)^\alpha(\partial\theta/\partial R)\, \tilde{c}_\beta \exp\{(i/\hbar) \int_\infty^R [H^a_{\beta\beta}-H^a_{\alpha\alpha}]\, \dot{R}^{-1}dR\} \ , \tag{2.12}$$

where $\alpha = 1$ or 2, $\beta = 1$ or 2 and $\beta \neq \alpha$.

In order to solve these equations in either representation we must specify R(t). The mean trajectory approximation (MTA) prescribes the use of Hamilton (or Newton) equations with the effective potential

$$V(R) = \sum_{i,j=1}^{2} c_i^* c_j H_{ij} \qquad (2.13)$$

In what follows we solve simultaneously the equation of motion for R(t) and that for the amplitudes c_α (or $\tilde{c}_\alpha$, in the adiabatic representation).

II.2. NUMERICAL RESULTS

We present here the mean trajectories, the occupation probabilities of the states 1 and 2, and the effective potential as functions of time, for various values of the Massey parameter λ. The results are compared to Nikitin's formula[3] and to those obtained by running trajectories on the lowest adiabatic state.

The relationship between the λ values used in these calculations and the incident kinetic energy is given in Table 2. The mass of the Na atom and the parameter values indicated in Table 1 were used to make the connection. We have $mv_o^2/2 = (m\Delta\varepsilon^2/2\hbar^2\alpha^2\lambda^2) = 3.30\ \lambda^{-2}$ (Hartree) $= 89.9\ \lambda^{-2}$ eV.

The numerical calculations consist of solving the differential equations (2.3) (for the diabatic representation) or (2.12) (for the adiabatic representation), simultaneously with Newton's equation with the effective potential Eq. (2.13).

The mean trajectory R(t) for a particle starting in state 1 is shown in Fig. 2. From each curve we can obtain the values of the following parameters: the position and the time at which the particle turns (R changes sign) and the times when the particle goes for the first and the second time through the diabatic crossing point R = 5. All these parameters characterizing the kinematics on the mean trajectory show interesting quantum behavior. If we were to run a Newtonian trajectory on the lower adiabatic state we would expect all the trajectories considered here to turn at approximately the same distance R, located on the sharp repulsive part of the surface. Fig. 1 places this value of R between 1.2 and 1.6. In Fig. 2 we see that the value of R at the turning point has the values 3.3, 2.15, 1.8 and 0.7 (for λ = 20, 10, 5 and 2, respectively). Furthermore, the times of the second crossing are 7.6, 10, 11.2 and 12.3 for λ = 20, 10, 5, 2, respectively); they have the striking feature that the low energy

particle (e.g. $\lambda = 20$) recrosses much earlier than the fast one (e.g. $\lambda = 2$).

The two effects are related, since the low energy particle reaches the second crossing first partly because it turns around earlier than the high energy one. These observations can both be rationalized as quantum effects introduced through the effective potential which depends, through the electronic amplitudes, on the incident energy (hence, on λ). As shown in Figs. (3.a)-(3.d) the effective potential can differ markedly from the adiabatic ones. Since we start with a particle in the diabatic state 1 the effective potential at large R resembles H_{11}. As the particle approaches the surface and the transition $1 \rightarrow 2$ starts taking place, the effective potential differs from both adiabatic ones. If the population of the adiabatic state 2 is larger than that of the state 1 the effective potential resembles H^a_{22}. This is roughly the case in Fig 3. where $\lambda = 2$ corresponds to a kinetic energy of 22.4 eV. Lowering the kinetic energy gets the effective potential closer to H^a_{11}. Since the effective potential can be computed only at points reached by trajectories the curve stops at the values of R corresponding to the turning point (given in Fig. 2). Finally, note that the effective potential for the incoming trajectory is different from the outgoing one; this happens because the amplitudes c_i are different on the two trajectories.

The reason why both the turning and the recrossing times go down with energy can be understood by looking at Figs (3.a) - (3.d). At the highest energy V_{eff} is close to H^a_{22}, while at low energy V_{eff} is close to H^a_{11}. Thus, an energetic particle has to travel a longer distance, both to turn around and recross, than a slow one.

The probability P^a_1 of remaining on the initial adiabatic

state Φ_1^a is plotted in Fig. 4, for four values of λ. All the curves change rather suddenly as the particle passes through the crossing region ($R \sim 5$). The magnitude of this change increases monotonically with λ^{-1}, that is with the kinetic energy. The largest kinetic energy gives the biggest drop in P_1^a. This correlates nicely with the fact that in Figs. (3.a) - (3.d) the effective potential V_{eff}, which starts by being close to H_{11}^a, crosses over to resemble H_{22}^a for small values of λ, but remains similar to H_{11}^a for $\lambda = 10$ or 20. The behavior of P_1^a at the second crossing is not a monotonic function of λ. For two values of λ (i.e. 20 and 5) P_1^a decreases at the second crossing, while for λ equal to 10 or 2, P_1^a increases at the second crossing. This suggests that the asymptotic value (i.e. the post collision value) of P_1^a oscillates with λ. That this is the case is seen in Fig. 5 where we plot the final values of P_2^a as a function of λ, for values of λ around $\lambda = 2.1$ (i.e. incident kinetic energy around 20.3 eV). On the same graph we plot the results of Nikitin's theory[3] which uses

$$P = 2P_{1\to2}(1-P_{1\to2}), \tag{2.14}$$

$$P_{1\to2} = \exp(-\lambda(1-\gamma))\ \{\sinh[\lambda(1+\gamma)]/\ \sinh[2\lambda]\} \tag{2.15}$$

and

$$\gamma = (1 + \beta^2)^{-1/2} \tag{2.16}$$

The Nikitin formula does not give rise to oscillations, but it goes smoothly through them. Reasonable qualitative agreement with our numerical results is obtained if Nikitin's equation for P is multiplied by

$$2\sin^2\left[\int_{t_1}^{t_f} [H_{11}^a\ (R(t)) - H_{22}^a\ (R(t))]dt/2\hbar + \phi\right] \tag{2.17}$$

where ϕ is an adjustable, time independent phase, t_1 is a pre-

collision time and t_T is the time at which the trajectory reaches the turning point; this factor is suggested by arguments similar to those made in the classic Stuckelberg paper and are not repeated here.[4]

In order to find the period of oscillation we use $dt = dR/|v|$, where $v = \dot{R}$, and the expressions for H_{11} and H_{22} given by the Eqs. (2.4). Assuming that $|v|$ is constant we obtain

$$I \equiv \int_{R_1}^{R} \frac{dR}{|v|\hbar} (H_{11}^a - H_{22}^a) =$$

$$(\hbar|v|)^{-1} \int_{R_1}^{R_t} \{4U_o \exp(-\alpha(R-R_o) - \Delta\epsilon)^2 + 16\beta^2 U_o^2 \exp(-2\alpha(R-R_o))\}^{1/2} dR \qquad (2.18)$$

Here I is the time dependent term in the argument of the sin function in the previous equation. Since the major contribution to this integral comes from values of R near the turning point, we neglect $\Delta\epsilon$. This allows us to perform the integral. Since R_1 is arbitrarily large we chose it so that all the terms $\exp(-\alpha R_1)$ are zero. After all these we obtain

$$I = -2U_o(1+\beta^2)^{1/2} (\lambda/\Delta\epsilon) \exp(\alpha R_o)$$

Thus $\sin^2(I+\phi)$ oscillates as a function of λ with a period of $2\pi\lambda/I$ (this is independent of λ!). The parameter values used in the present work lead, when inserted in the above equation to a period of 0.081 which is close to that given by the numerical calculations. This might seem gratifying, since such oscillations are in principle observable and the simple analysis presented above links their period to the asymptotic gap $\Delta\epsilon$, the binding energy of the ion U_o, the strength of the coupling β, and the range of the potential α^{-1}. Unfortunately in most surface

science problems the phase will be randomized to some extent by inelastic processes and this will smooth out, or perhaps even wipe out, the oscillations.

The behavior of a system which starts in the adiabatic state 2 is shown in Figures 6, 7.a - 7.d and 8. The discussion of these results follows along the lines of the case when the particle starts in the state 1, and it is therefore omitted.

A comparison between the mean trajectory approximation and a theory in which the particle is propagated on the adiabatic surface 2 (the initial state is 2) is presented in Figs. 9.a - 9.d. The fact that the largest differences between the two theories are obtained for the smaller values of λ (i.e. $\lambda = 2$ and 5) might seem surprising, since, in general, one expects the two theories to differ less at high energy. However, an examination of the Figures 7.a - 7.d shows the reason for this result: the effective potential at small values of λ resembles H^a_{11} fairly closely, and differs from H^a_{22}; thus for small λ the mean trajectory differs most from a classical trajectory on H^a_{22}. This discrepancy between H^a_{22} and V_{eff} occurs because (Fig. 8) P^a_2 goes down at the first crossing for $\lambda = 2$ and $\lambda = 5$ much more than for $\lambda = 10$ or 20. Thus the effective surface switches, from being close to H^a_{22} prior to the first crossing, to becoming close to H^a_{11}.

If we attempt to apply Nikitin's formula we must take into account the fact that the velocity in the region where the two states interact strongly differs from the incident velocity. We include this effect by using Nikitin's formula with $\lambda^* = \Delta\varepsilon/\hbar\alpha v_c$, instead of $\lambda = \Delta\varepsilon/\hbar\alpha v_o$, where v_c is the velocity at the crossing point. This is given by $mv_c^2 = mv_c^2 - \Delta\varepsilon$ and as a result λ^* can be written as $\lambda^* = \lambda(1-\delta\lambda^2)^{-1/2}$, with $\delta = (\hbar\alpha)^2/m\Delta\varepsilon$. The transition probability after the first crossing is now given by

$$P_{2\to1} = \exp[-\lambda^*(1-\gamma)][\sinh \lambda^*(1+\gamma)]/[\sinh 2\lambda^*] \qquad (2.19)$$

with γ defined by (2.16). In Fig. 10 we show the dependence of $P_{2\to1}$ on λ given by the mean trajectory approximation (broken line) and by Eq. (2.19) (full line), for several coupling strengths β. The quantities λ_1 and λ_2 marked on the graphs are defined by $\lambda_1 = \Delta\varepsilon/\hbar\alpha v_1$ and $\lambda_2 = \Delta\varepsilon/\hbar\alpha v_2$ where v_1 corresponds to a kinetic energy equal to the asymptotic mismatch $\Delta\varepsilon$ (i.e. $v_1 = (2\Delta\varepsilon/m)^{1/2}$) and v_2 to a kinetic energy equal to the difference between the potential energy at the crossing point and the asymptotic energy of the lower energy curve (i.e. $v_2 = (\Delta\varepsilon/m)^{1/2}$). Nikitin's formula for $P_{2\to1}$ deviates only slightly from the mean trajectory values as λ exceeds λ_1. From Nikitin formula $P_{1\to2} = 0$ if $\lambda \geq \lambda_2$ while the mean trajectory calculations give small, finite values for $P_{1\to2}$ if $\lambda > \lambda_2$ which go to zero as λ is increased.

Nikitin's formula is further improved if we use in Eq. 2.19 $\lambda^{**} = \Delta\varepsilon/\hbar\alpha v_p$ instead of λ^*, where v_p is obtained from

$$mv_p^2/2 + H_{22}^a(R_p) = mv_o^2/2 - \Delta\varepsilon/2 \qquad (2.20)$$

and R_p is the position where $\partial\theta(R)/\partial R$ is maximum. For the model used here (i.e. Eqs. (2.4) $R_p = R_o + \alpha^{-1} \ln[4(1+\beta^2)^{1/2} W_o/\Delta\varepsilon]$, with R_o is defined by (2.4). These lead to

$$\lambda^{**} = \lambda(1 - \tilde{\delta}\lambda^2)^{-1/2} \qquad (2.21)$$

and

$$\tilde{\delta} = \delta[1 - [2(1-\gamma)]^{1/2} + (\gamma^2/16)(\Delta\varepsilon/U_o)(R_o/R_p)] . \qquad (2.22)$$

Using Eq. (2.19) with λ^{**} instead of λ^* gives almost perfect agreement with the mean trajectory approximation.

Unfortunately $P_{2\to1}$ is not measurable and the use of

Nikitin's formula to compute P_1^a, the probability that the system ends up in the adiabatic state 1 after having started in state 1, can be done with moderate success only after a correction for interference effects are made. To do this we multiply Nikitin's formula

$$P_1^a = 2P_{2\to1}(1-P_{2\to1}) \tag{2.23}$$

with the factor given by Eq. (2.17) which includes interference effects. The computation of $P_{2\to1}$ uses Eq. (2.19) with λ^{**} instead of λ^*. We use this corrected formula for a qualitative discussion of our numerical results and for making crude estimates.

In Figs. 11 and 12 we show the mean trajectory, results for P_1^a (full lines), together with the results obtained by running a trajectory on H_{22}^a (broken lines) and those given by Eq. (2.23) uncorrected for interference (i.e. Eq. (2.23) without multiplying it with (2.17). We see that as the coupling constant β and the incident kinetic energies are decreased the results obtained with the mean trajectory approximation differ markedly from those obtained by running a trajectory on H_{22}^a. This happens because the mean potential differs substantially from H_{22}^a. Qualitatively this can be understood as follows: since β is small the diabatic states are weakly coupled and the system tends to remain on its initial diabatic state. In the present case the system starts on H_{22} (which for large R coincides with H_{22}^a) and tends to stay on it. Since for small values of R $H_{22} \simeq H_{11}^a$ this means that the system tends to undergo a transition (in the adiabatic picture) from H_{22}^a to H_{11}^a. The mean potential, which is initially equal to H_{22}^a, begins to resemble H_{11}^a more than H_{22}^a. Thus after the crossing point $V_{eff} = H_{11}^a$ and therefore the calculation using H_{22}^a to obtain the trajectory leads to results which are very different from the mean trajectory ones.

In the remainder of this section we investigate a remarkable phenomenon that takes place for small β values. It is clear that the effective potential varies in time as driven by the quantum amplitudes c_i. Imagine a trajectory whose initial total energy is close to the maximum of H^a_{22}. If a transition to the adiabatic state 1 occurs the effective potential changes into a mix of H^a_{11} and H^a_{22}. Since $H^a_{11} > H^a_{22}$ this can have the effect of making the barrier of V_{eff} larger than the barrier of H^a_{22} and the total initial energy of the particle. It is thus possible that a trajectory that would pass over H^a_{22} - if that surface was used in Newton's equation - can be reflected by $V_{eff}(R)$ since that potential will have a larger barrier. Furthermore, a trajectory which passed over the barrier of V_{eff} in its way to the surface may be trapped in its way out by a surge in V_{eff}, caused by an increase of the transition amplitude to the upper adiabatic state 1. Due to the all or nothing character of the classical reflection process we expect to see some sudden changes in the behavior of the system as we vary β (or λ) through the range in which such a process can take place. The numerical results show the onset of a remarkable behavior: within our ability to resolve the issue the transition probability P^a_1 becomes a random, discontinuous function of λ. We expect the phenomena mentioned above to take place when the effective potential exceeds to total energy of the particle. After the second crossing the effective potential is roughly $1/2\ \Delta\epsilon P^a_1 - (\Delta\epsilon/2)(1-P^a_1) = \Delta\epsilon(P^a_1-1/2)$ and the asymptotic energy conservation condition is $mv_o^2/2 \sim 1/2\ \Delta\epsilon = mv_f^2/2 + \Delta\epsilon(P^a_1 - 1/2)$. It is possible to obtain zero final velocity $\Delta\epsilon(P^a_1 - 1/2) \geq mv_o^2/2 - \Delta\epsilon/2$. This leads to

$$P^a_1 \geq mv_o^2/2\Delta\epsilon = (2\delta\lambda^2)^{-1} \quad . \qquad (2.24)$$

This equation permits us to estimate under what conditions we can expect the effective potential to turn the particle back towards the surface after the second crossing.

In Fig. 13 we plot the maximum value obtained max P_1^a of P_1^a obtained from

$$P_1^{a,max} = 4P_{2\to1}\,(1 - P_{2\to1}) \quad , \qquad (2.25)$$

with $P_{2\to1}$ given by Eq. (2.19). The factor of 4 appears because the Nikitin formula corrected to include interference is $P_1^a = 4\,P_{2\to1}\,(1 - P_{21})\,\sin^2\theta$ and the maximum value is obtained by taking the sin equal to one. The broken curve is $(26\lambda^2)^{-1}$ and the full lines are the maximum values of P_1^a, computed as described above, for various values of β. For $\beta = 0.1$ the broken and the full lines cross and the condition (2.24) is satisfied in the range of λ values indicated by arrows (for $\beta = 0.1$). This is roughly the range (λ_1, λ_2), where λ_1 and λ_2 were defined earlier. For higher values of coupling constant β (2.24) is not satisfied.

While we have used approximate formulae to obtain the plots in Fig. 13 they give us a fairly reliable hint concerning the parameter region where we should look for unusual behavior in the mean trajectory results. In Fig. 14a we show the dependence of P_2^a, given by the mean trajectory approximation, for $\beta = 0.1$ and $\lambda = 30$, 30.015 and 30.020. $P_2^a(t)$ is the probability that the particle is on the adiabatic state 2 at time t. The horizontal broken line indicates the values of P_2^a below which the condition (2.24) is satisfied. For $\lambda = 30$ and 30.015 the condition is not satisfied at any time and the behavior of P_2^a is normal: at $t \sim 7$ the particle undergoes its first crossing and at $t \sim 11$ the second one.

Since the asymptotic value of P_2^a oscillates as a function of λ the two curves go to different asymptotic values. The curve $\lambda = 30.02$ behaves quite differently. After the second crossing at $(t \sim 11)$ P_1^a satisfied Eq. (2.24) and the effective potential

exceeds the total energy of particle. Therefore the particle, which is moving away from the surface, is turned back and undergoes a third crossing at t ~ 38 which takes P_2^a above the broken line; the fourth crossing lifts P_2^a even higher so the energy of the particle exceeds that of the effective potential and the particle escapes. This interpretation is substantiated by the trajectory plots shown in Fig. 14b, for the same conditions. The crossing point is at R = 5 and the trajectory corresponding to λ = 30.02 crosses it four times. In Fig. 14c we show the effective potential for λ = 30.02, plotted together with the adiabatic potentials (broken lines). As the particle approaches the surface the effective potential is the curve indicated by (1). After the crossing point R=5.0 the potential has the form shown as (2). This curve stops at the turning point and the height of that point equals the total energy of the particle (since there the velocity is zero). The potential (2) is half way between H_{11}^a and H_{22}^a and it is repulsive. After the turning point the probability P_1^a does not change until the particle reaches crossing point and the potential remains unchanged (i.e. it is given by (2)). At the crossing point the probability changes and the effective potential (3) resembles more H_{11}^a and it becomes attractive. At R a bit larger than 7 the particle reaches a turning point and goes back towards the wall. At the crossing the probability changes again and the effective potential is given by curve (4). This resembles more the potential H_{22}^a than the effective potential (2) which acted on the particle when it first approached the wall. The particle hits the wall and turns around and the effective potential is still (4) since P_1^a is not changing. At the turning point P_1^a becomes very small and the effective potential (5) is repulsive (since it is largely composed of H_{22}^a) and the particle escapes.

To investigate this phenomenon in more detail by calculating the asymptotic values of P_1^a as a function of λ, for λ in the range [30.00. 30.2] in which the unusual behavior takes

place. The results are represented in Fig. 15. In Fig. 15a we show by full lines the mean trajectory results for the case when the behavior is normal. P_1^a in that range is a continuous function of λ. The circles represent results obtained with the mean trajectory approximation in the range of λ values where multiple trajectories occur. The numbers near the circles indicate how many times the trajectory was turned back towards the wall. If the number is 1 the trajectory hit the wall twice, if the number is 4 then the the wall was hit five times, etc. The broken lines show the results for P_1^a at the time when the particle is moving away from the surface hits the wall for the first time and hits the turning point that will send it back towards the surface for a second collision. The horizontal line is given by the Nikitin formula, uncorrected for interference. In order to find whether the circles follow a pattern we carried out mean trajectory calculations in a very narrow range $\lambda\varepsilon[30.01, 30.05]$. Even with this very high resolution we still find that the values of P_1^a represented by the circles seem to originate from a <u>discontinuous</u> function $f(\lambda)$(i.e. $P_1^a = f(\lambda)$). In Fig. 16 we show that the phenomenon appears for other values of λ.

IV DISCUSSION

The mean trajectory approximation introduces, through the mean potential, some quantum effects into the "classical" trajectory. To understand how such effects work and how we can improve their treatment it is useful to recall one of the derivations of the MTA. We have shown that we can generate MTA by running a narrow wave packet on the two state systems. This is done by chosing a wave function of the form

$$\psi(x,R;t) = G(R;t)\{c_1\Phi_1(x,R(t)) + c_2\Phi_2(x,R(t))\}$$

where G(R;t) is a Gaussian wave packet. Using a method developed by Heller[5] we can generate equations for the motion of the center of the wave packet which turn out to be the mean trajectory equation. These equations will attempt to mimic the quantum motion of the packet. The temporary trapping of the particle can be rationalized in terms of this picture as follows. If the packet passes the crossing point and P_1^a is very small, it will move like a classical particle on the lower adiabatic state H_{22}^a. Let us assume that the particle hits the surface and when it comes back P_1^a becomes large. The packet now moves mostly on the upper state H_{11}^a and it is trapped in its potential well. As it rattles around it passes through the crossing point and if P_1^a stays high the packet remains trapped; if P_1^a becomes small the packet goes on H_{22}^a and it escapes (if it happens to move away from the wall) or it collides with the wall (if it happens to move towards it). If the collision with the wall takes place the particle turns around, it may repeat the above sequence (if P_1^a becomes large), or it may get away (if P_1^a stays small).

Attempting to describe the motion of the particle by using one packet agrees in a superficial way, with our intuition. We want to treat the atom motion classically and it is well known that we can achieve that by taking a nuclear wave function which

is a narrow Gaussian. We obtain then one trajectory (i.e. the mean trajectory) and this is in agreement with our classical prejudices that one trajectory should describe the motion of one atom.

However, if we forget that we have ever heard of the Newtonian classical mechanics and only think of it as a computationally advantageous limit of quantum mechanics (which is taken by using narrow Gaussian wave packets) than we will generate an entirely different picture. Since quantum wave function is of the form

$$\psi(x_1 R;t) = x_1(R)\Phi_1(x;R) + x_2(R)\Phi_2(x;R)$$

where x_1 and x_2 are nuclear wave functions, we should replace x_1 (R) and x_2(R) with two distinct Gaussians. By forcing them to be narrow we can use time dependent Schrodinger equation to generate two classically looking equations for the centers of the two Gaussians. We have now two trajectories, one for each electronic state. The Guassian G_1 associated with the electronic state Φ_1, moves on a potential that resembles H_{11} and G_2 on one which resembles H_{22}. However, the two trajectories are coupled by a potential which is large whenever the two Gaussians overlap and whose magnitude depends on the coupling H_{12}.

The picture emerging from such a description is more complex and more successful in the sense that it provides a classical like description which contains most of the important quantum effects. The occupation probability is given by the amplitudes of the Gaussians and if P_1 is large then $(G_1)^2$ is large and $(G_2)^2$ is small. Asymptotically the two packets emerge with two different momentum distributions: the one moving on the upper state has a smaller mean momentum than the one moving on the bottom state. This reflects the fact the particles emerging on one electronic state have a different kinetic energy than

those emerging on the other. MTA, on the other hand gives a kinetic energy which is the average of this distribution.

Furthermore, the trajectory running on state 1 and that running on state 2 have different turning points, which better mimic the behavior of the two nuclear wave functions. MTA has one turning point which is an average of that of the two trajectories.

A more striking demonstration of the need for double trajectories can be made when we include a decay mechanism by which the particle can lose energy by exciting phonons or electrons in the solid. The trajectory running on H_{11} can be trapped (forever) if it loses energy to excite the solid; the one running on H_{22} cannot be trapped since the state 2 is repulsive. Thus the behavior of the two trajectories is extremely different. If a mean trajectory is used for such situations it will either get trapped or it will escape since it will give the average behavior of the two trajectories. If the amplitude of the escaping Gaussian is the larger one than the mean trajectory will escape; in the opposite case it will get trapped. It is unlikely that the average behavior will mimic faithfully the more correct, "bimodal" behavior of the two trajectories model. How well MTA compares to a double trajectory theory can be decided only by a detailed numerical investigation, which is now in progress.[6]

Acknowledgements

This work was supported by the National Science Foundation (NSF CHE 82-06130) and the Office of Naval Research. We have benefited from discussion with Eric Heller and Abe Nitzan.

References.

1. J. C. Tully, Phys. Rev. B, 16, 4324 (1977); J. Delos, W. Thorson and S. Knudson, Phys. Rev. A, 6, 709 (1972); C. Melius and W. Goddard III, Phys. Rev. A, 10, (1974); P. Pechukas, Phys. Rev. 181, 174 (1969).

2. S. Sawada, A. Nitzan and H. Metiu, Phys. Rev. B, to be published.

3. E. E. Nikitin, Discussion Faraday Soc. 33, 14 (1962); Theory of elementary atomic and molecular processes in gases (Clarendon, Oxford, 1974).

4. E. C. G. Stueckelberg, Helv. Phys. Acta 5, 369 (1932).

5. E. Heller, J. Chem. Phys. 62, 1544 (1975); ibid. 64, 63 (1976).

6. S. Sawada and H. Metiu, to be published.

FIGURE CAPTIONS

1. The diabatic and adiabatic energy surfaces and the coupling used in the present calculations. For the definitions see Eqs. (2.4) and (2.7)-(2.9).

2. The mean trajectories (atom-surface distance as a function of time) for various values of the Massey parameter λ (defined by Eq. (2.5)) or, equivalently, incident kinetic energy K (in eV). The arrows mark the turning points. The intersection with the curve R = 5 gives the times (marked on the figure) when the particle passes through the crossing point of the diabatic curves. The turning points are the points where R changes direction; the turning distances are given near the horizontal arrows and the turning times near the vertical ones.

3. The effective potentials V_{eff} (full lines) for various values of the Massey parameter λ as a function of the surface-atom distance. The arrows mark the direction of particle motion. The adiabatic energy surfaces, H^a_{11} and H^a_{22} are given by the broken lines.

4. The probability P^a_1 of remaining on the adiabatic state ϕ^a_1 as a function of time, for various values of the Massey paramter λ.

5. The asymptotic value of the probability P^a_2 that the system starts in the adiabatic state 1 and emerges in the adiabatic state 2, as a function of λ. The solid line gives the MTA results and the broken line those of the Nikitin theory.

6. The same as Fig. 2 except that the system starts in the adiabatic state 2.

7. The same as Fig. 3 except that the system starts in state 2.

8. The same as Fig. 4 except that the system starts in state 2.

9. The probabilities P_2^a that the system starts and stays on state 2, as functions of time. The full line gives the results of the trajectory approximation with the adiabatic potential H_{22}^a; the broken line give the mean trajectory approximation (MTA) results.

10. The transition probabilities $P_{2\to1}$ as a function of the Massey parameter λ for several coupling strengths β. The full lines give the results of Nikitin's theory, and the broken lines give the MTA results. λ_1 and λ_2, are defined in the text.

11. The asymptotic values of probability P_1^a (the probability that the particle starts on state 2 and emerges on state 1) as a function of λ for $\beta = 0.3$ given by the mean trajectory approximation (full line), the trajectory approximation with the adiabatic potential H_{22}^a (broken line) and the Nikitin's theory (chain line).

12. The same as Fig. 11 except $\beta = 0.15$.

13. The maximum asymptotic values of probability P_1^a as functions of λ for various values of β (full lines) and the value of $(2\delta\lambda^2)^{-1}$ (broken line).

14a. The probability P_2^a (that the particle starts and remains on state 2) as a function of time for several values of λ (solid lines), as computed by MTA. The broken line indicates the values of P_2^a below which the condition (2.24) is satisfied.

14b. The mean trajectories for several values of λ (full lines). The broken line indicates the crossing point.

14c. The effective potential for $\lambda = 30.02$ (full line) and the adiabatic potentials (broken lines). The numbers (1) - (5) indicates the time sequence in which the particle moves on the effective potential (see the text).

15a. The asymptotic values of the probability P_1^a (that the particle starts on state and emerges on state 1) as a function of λ given by the mean trajectory approximation (full curve and circles) and by Nikitin's theory (-·-·-). The numbers near the circles indicate how many times the trajectory turned back towards the wall. The broken lines show the results for P_1^a at the time when the particle hits the turning point that will send it back towards the surface for a second collision (see text).

15b. Same as Fig. 15a.

16a. Same as Fig. 15a.

16b. Same as Fig. 16a. The arrow indicates the value of λ for which $1/2\ mv_0^2 - \Delta\epsilon/2 = H_{22}^a(R=R_p)$ so that the particle turns back without the collision with the wall.

16c. Same as Fig. 16b.

Table 1. The values of the parameters used in the present calculations

U_o	= 0.025 Hartree	0.68 eV
$\Delta\varepsilon$	= 0.005 Hartree	0.136 eV
α	= 0.4 Bohr radius^{-1}	0.756 Å^{-1}
α^{-1}	= 2.5 Bohr radius	1.32 Å
R_o	= 5.0 Bohr radius	2.64 Å
β	= 0.1, 0.15, 0.3	
m	= 42300 (in the atomic unit)	
δ	= $\hbar^2\alpha^2/m\Delta\varepsilon = 7.56 \times 10^{-4}$	

Table 2. The relationship between the values of λ and the incident kinetic energy

λ	Incident Kinetic Energy (Hartree)	(eV)
2	0.825	22.4
5	0.132	3.59
10	0.033	0.8976
20	0.00825	0.224
30	0.00367	0.0999
36	0.00255	0.0694

$mV_o^2/2 = \Delta E/2\delta\lambda^2 = 3.30/\lambda^2$ Hartree $= 89.9/\lambda^2$ eV

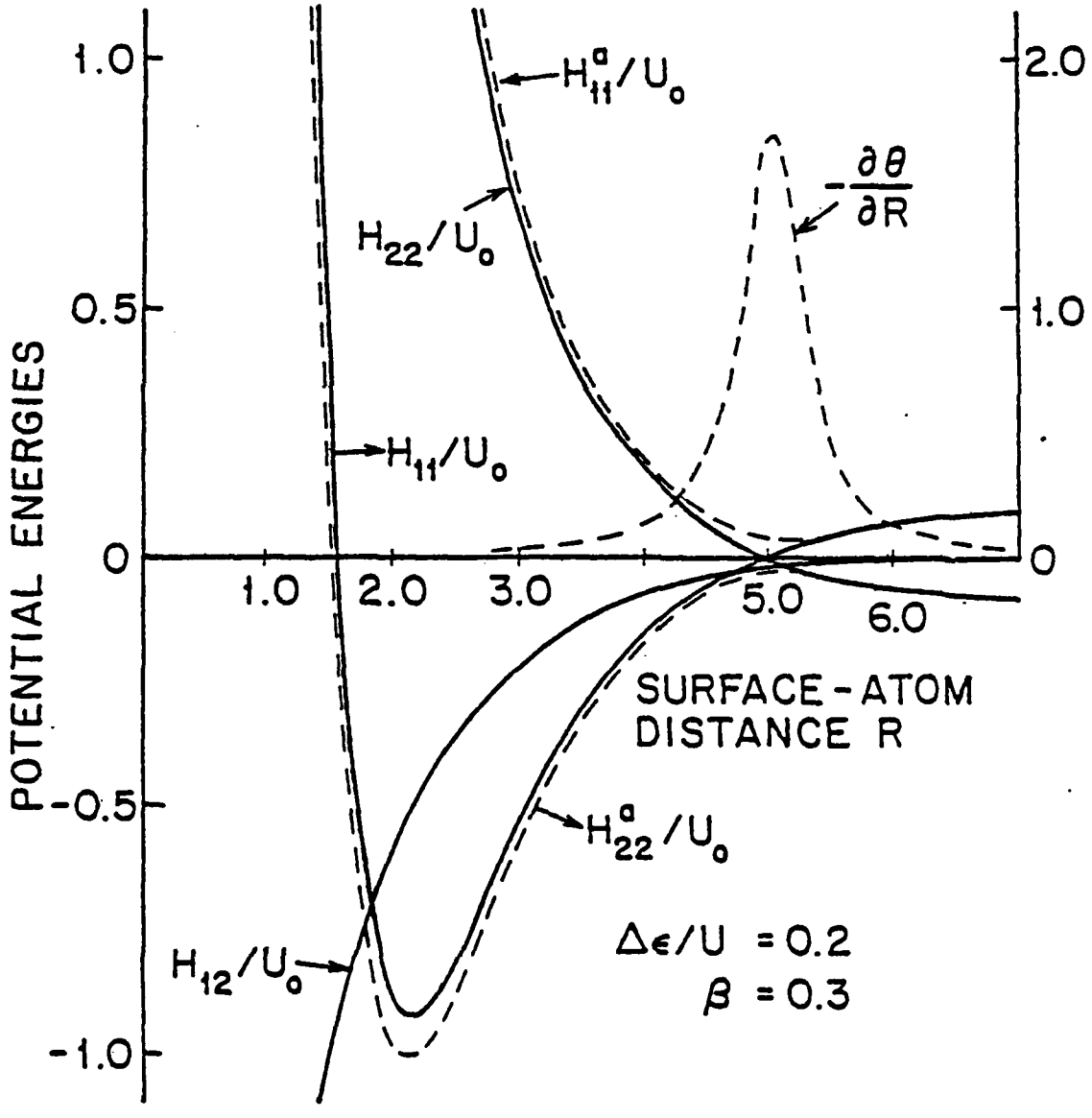
1.0
0.5
0
-0.5
-1.0
2.0
1.0
0
1.0
2.0
3.0
5.0
6.0
POTENTIAL ENERGIES
SURFACE-ATOM DISTANCE R
H^a_{11}/U_o
H_{22}/U_o
$-\frac{\partial\theta}{\partial R}$
H_{11}/U_o
H^a_{22}/U_o
H_{12}/U_o
$\Delta\epsilon/U = 0.2$
$\beta = 0.3$

Fig. 1

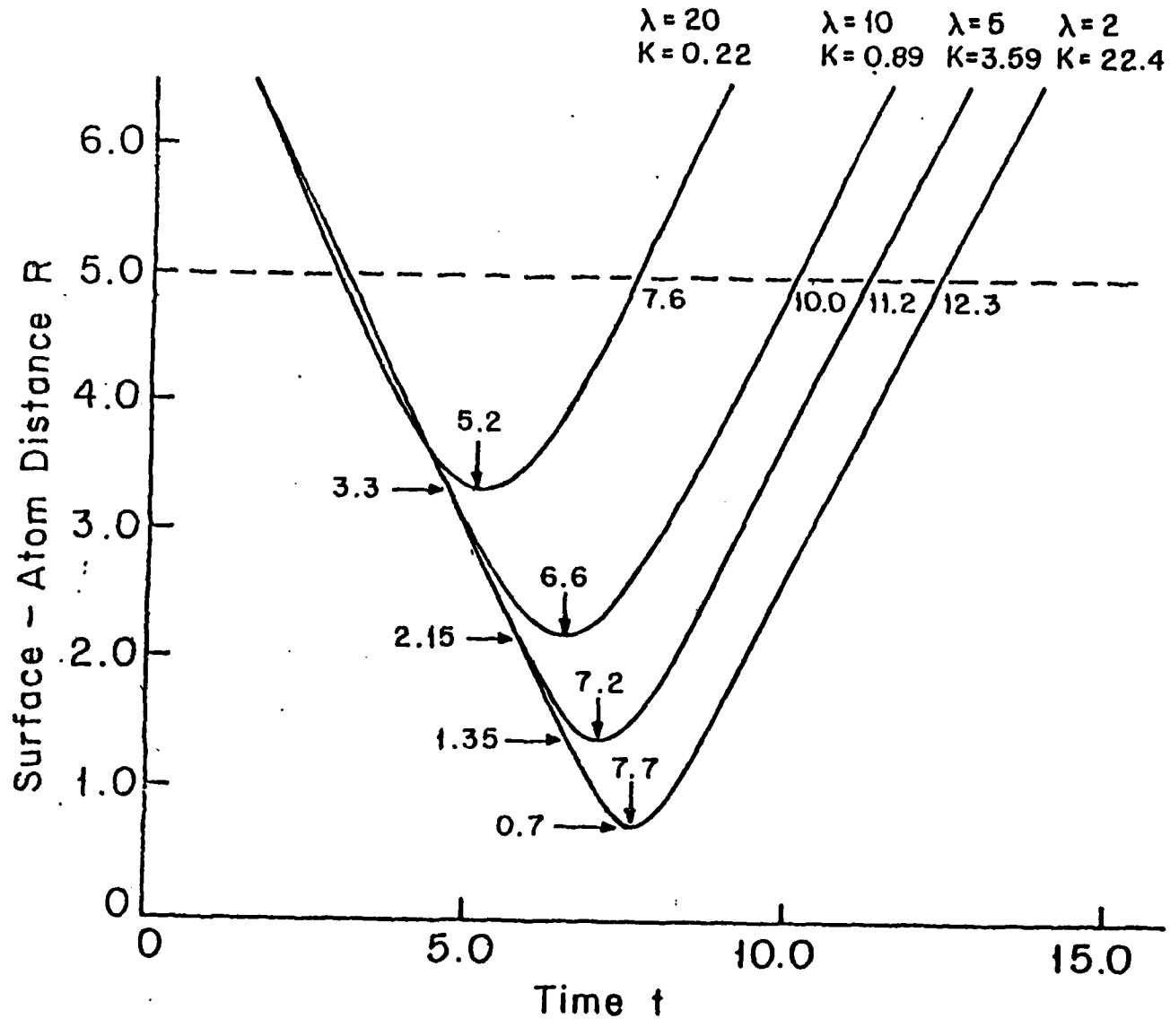
λ = 20
K = 0.22
λ = 10
K = 0.89
λ = 5
K = 3.59
λ = 2
K = 22.4
6.0
5.0
4.0
3.0
2.0
1.0
0
Surface – Atom Distance R
7.6
10.0
11.2
12.3
5.2
3.3
6.6
2.15
7.2
1.35
7.7
0.7
0
5.0
10.0
15.0
Time t

Fig 2

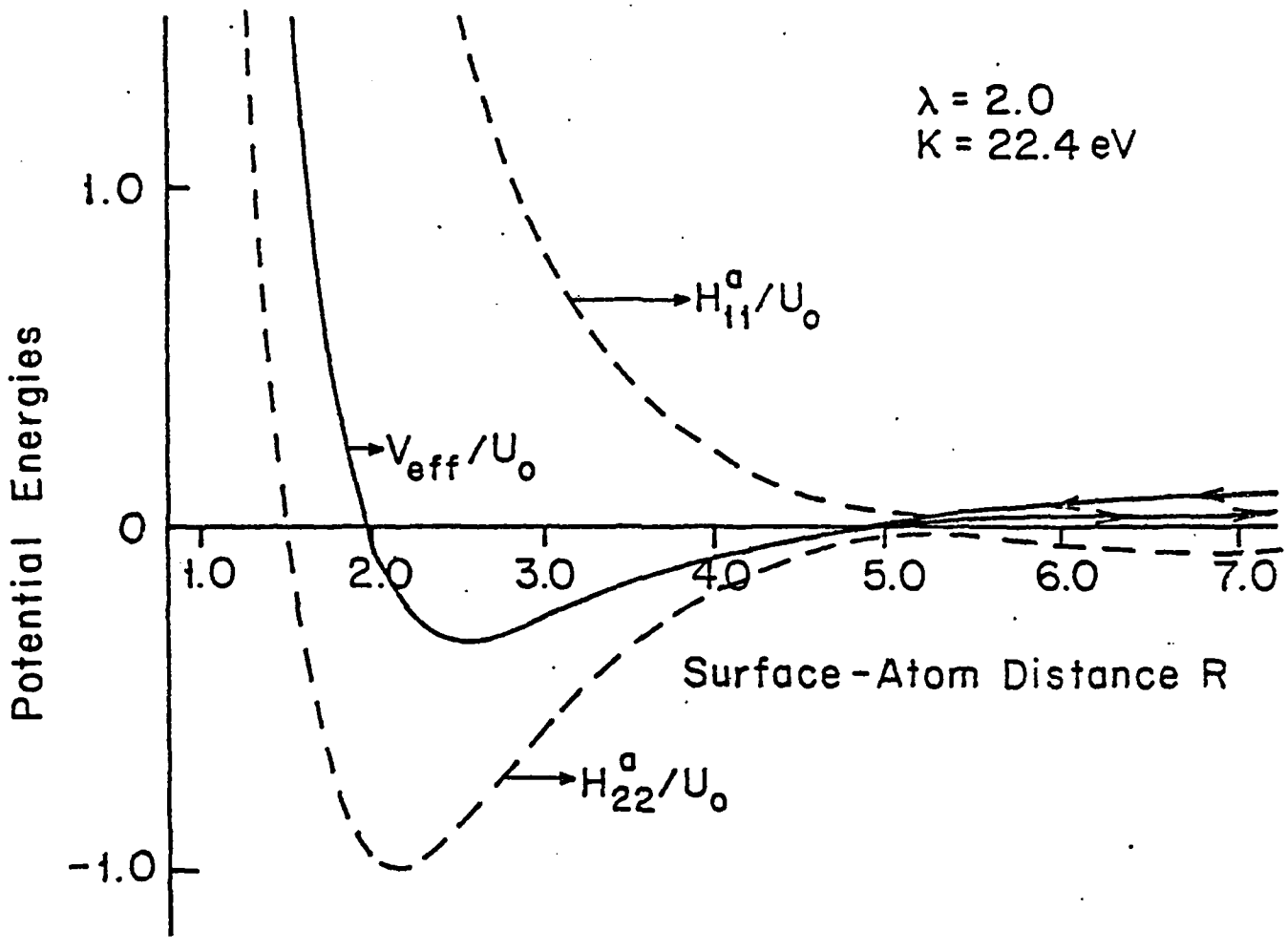
λ = 2.0
K = 22.4 eV
1.0
0
-1.0
Potential Energies
H^a_{11}/U_o
V_{eff}/U_o
H^a_{22}/U_o
1.0
2.0
3.0
4.0
5.0
6.0
7.0
Surface-Atom Distance R

Fig. 3a

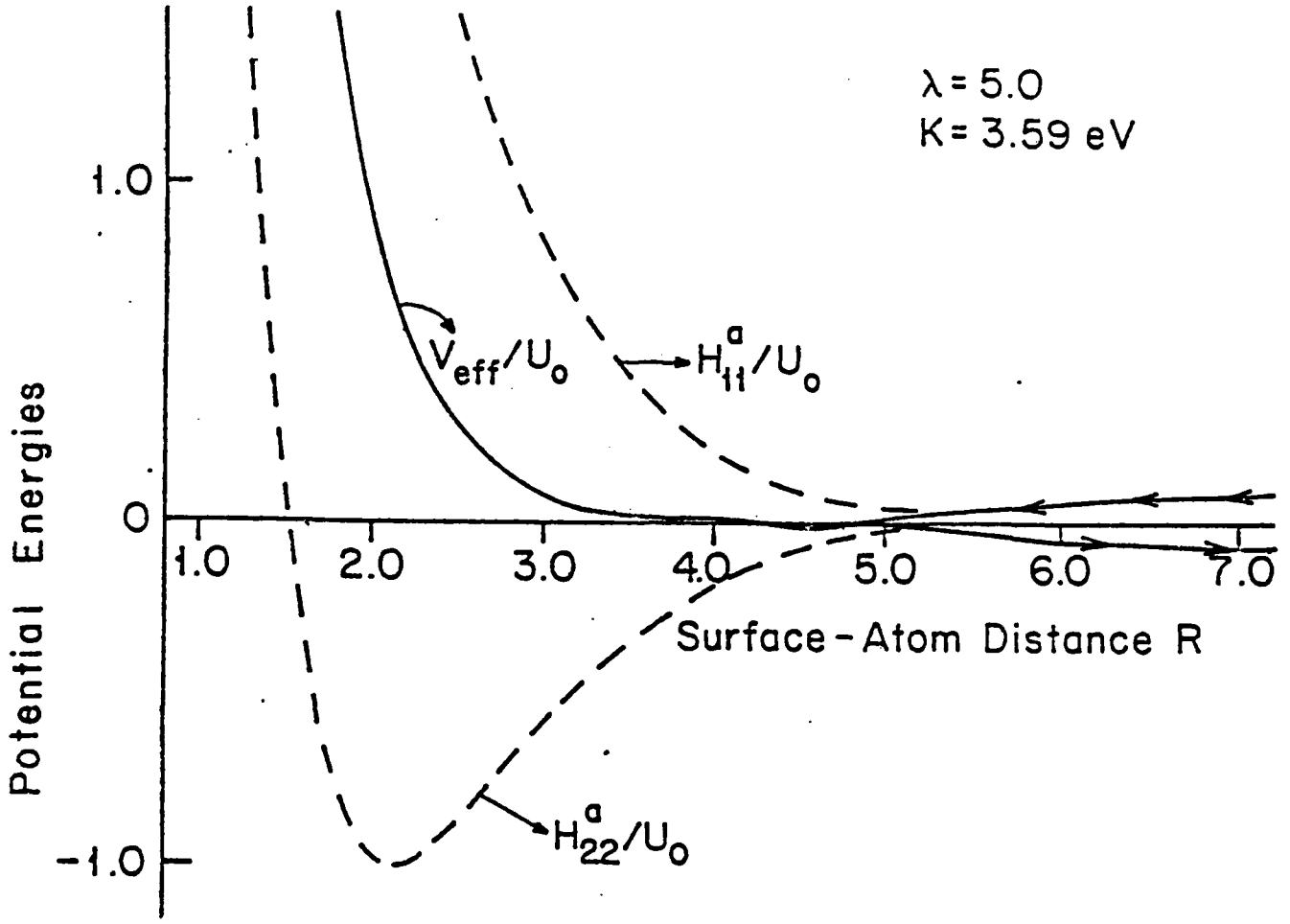
λ = 5.0
K = 3.59 eV
1.0
0
-1.0
Potential Energies
V_{eff}/U_o
H^a_{11}/U_o
H^a_{22}/U_o
1.0
2.0
3.0
4.0
5.0
6.0
7.0
Surface - Atom Distance R

Fig. 3b

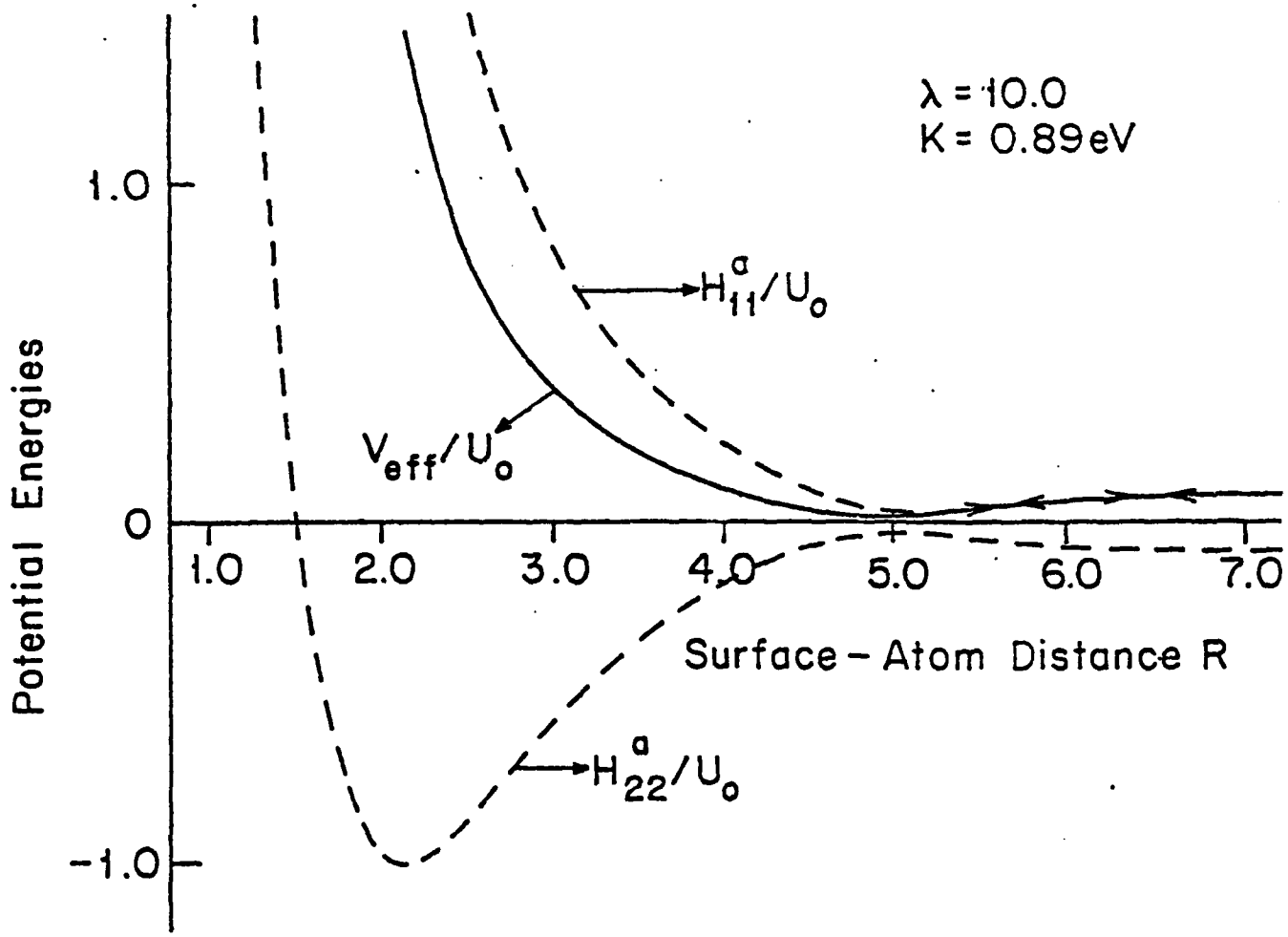
λ = 10.0
K = 0.89eV
1.0
0
-1.0
Potential Energies
H^a_{11}/U_o
V_{eff}/U_o
H^a_{22}/U_o
1.0
2.0
3.0
4.0
5.0
6.0
7.0
Surface – Atom Distance R

Fig 3c

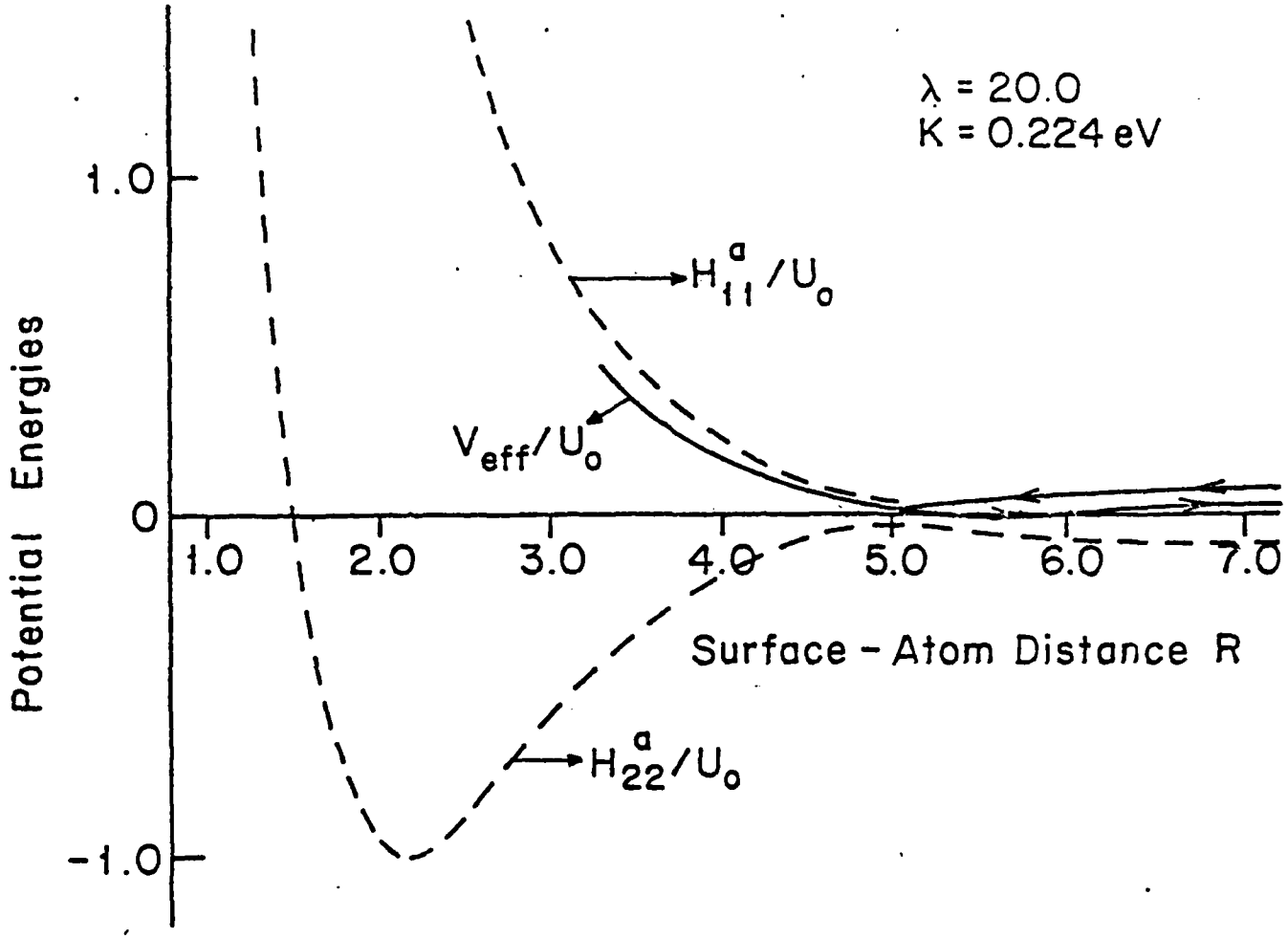
λ = 20.0
K = 0.224 eV
1.0
0
-1.0
H_{11}^a/U_o
V_{eff}/U_o
H_{22}^a/U_o
Potential Energies
1.0
2.0
3.0
4.0
5.0
6.0
7.0
Surface - Atom Distance R

Fig. 3c

Fig. 1

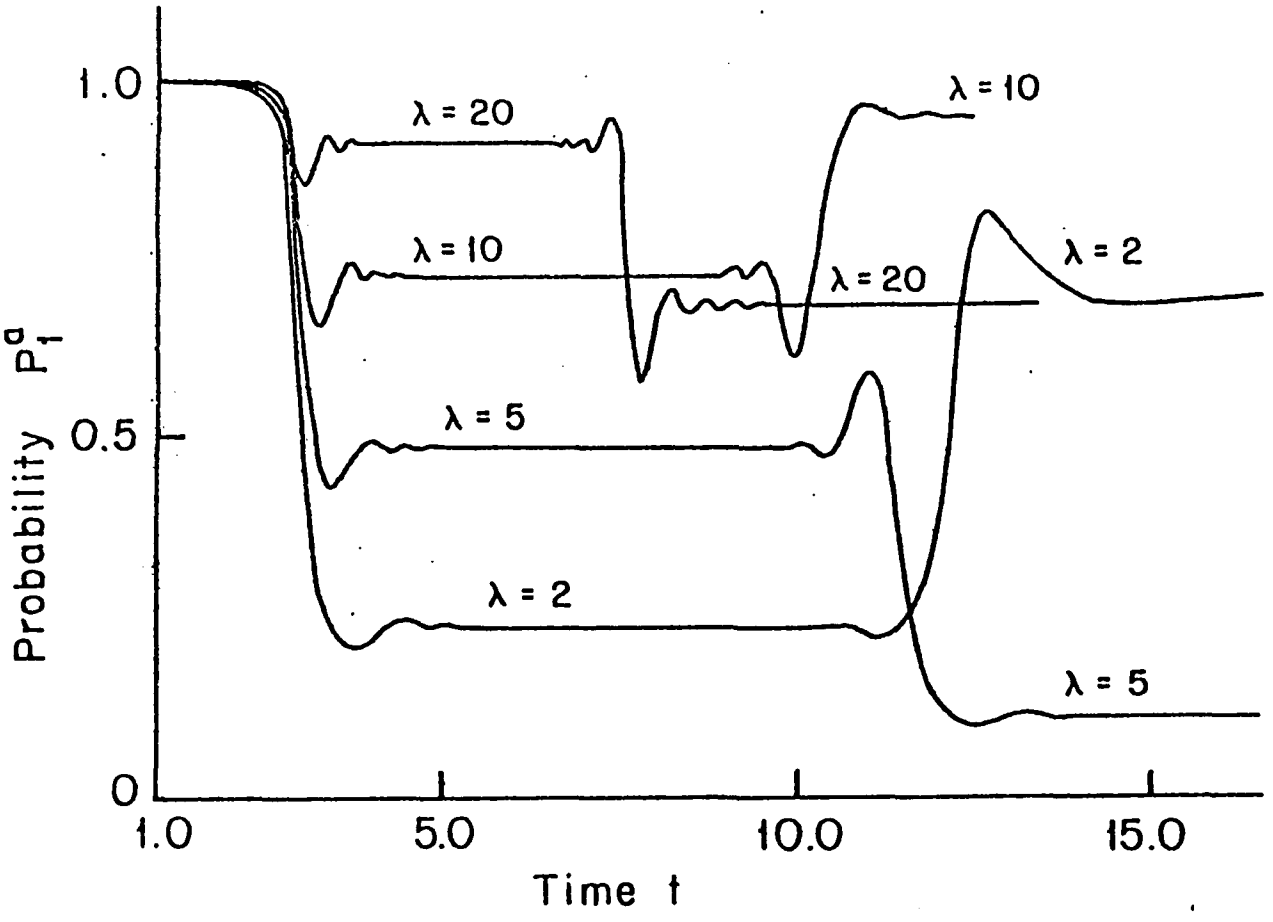
1.0
0.5
0
Probability P_1^a
λ = 20
λ = 10
λ = 5
λ = 2
λ = 10
λ = 20
λ = 2
λ = 5
1.0
5.0
10.0
15.0
Time t

Fig. 5

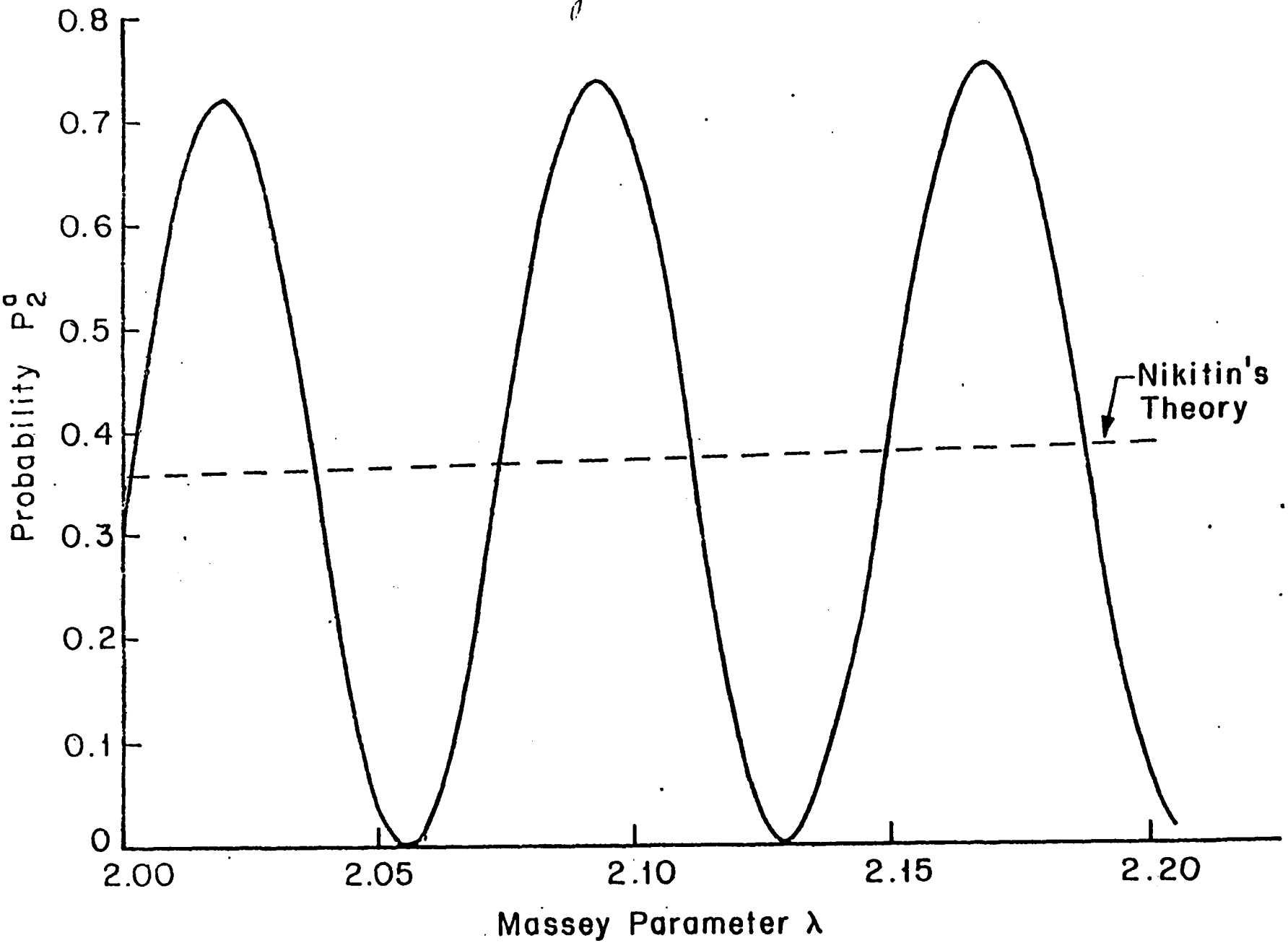
0.8
0.7
0.6
0.5
0.4
0.3
0.2
0.1
0
Probability P_2^a
Nikitin's Theory
2.00
2.05
2.10
2.15
2.20
Massey Parameter λ

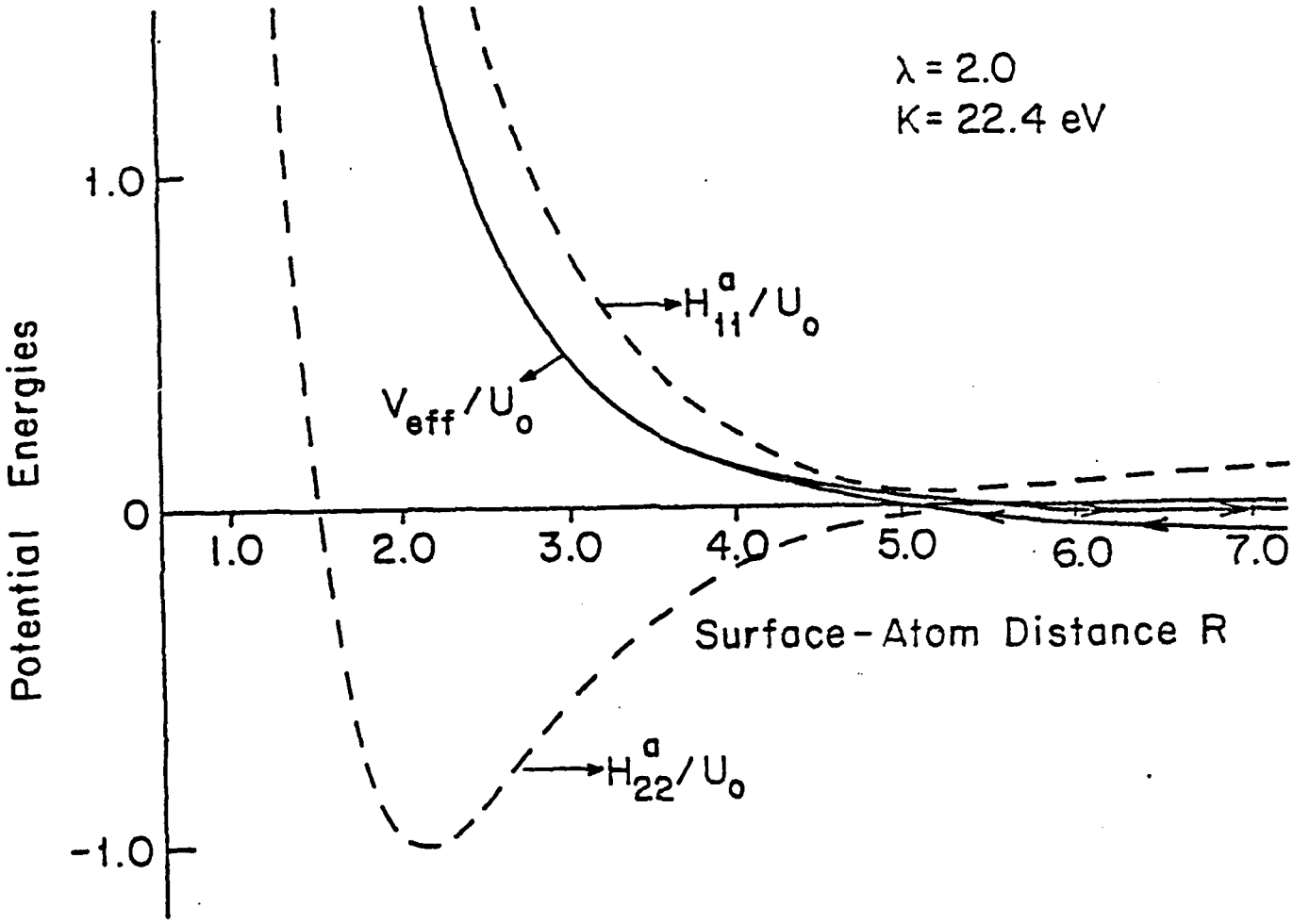
λ = 2.0
K = 22.4 eV
1.0
0
-1.0
Potential Energies
H^a_{11}/U_o
V_{eff}/U_o
H^a_{22}/U_o
1.0
2.0
3.0
4.0
5.0
6.0
7.0
Surface-Atom Distance R

Fig. 7a

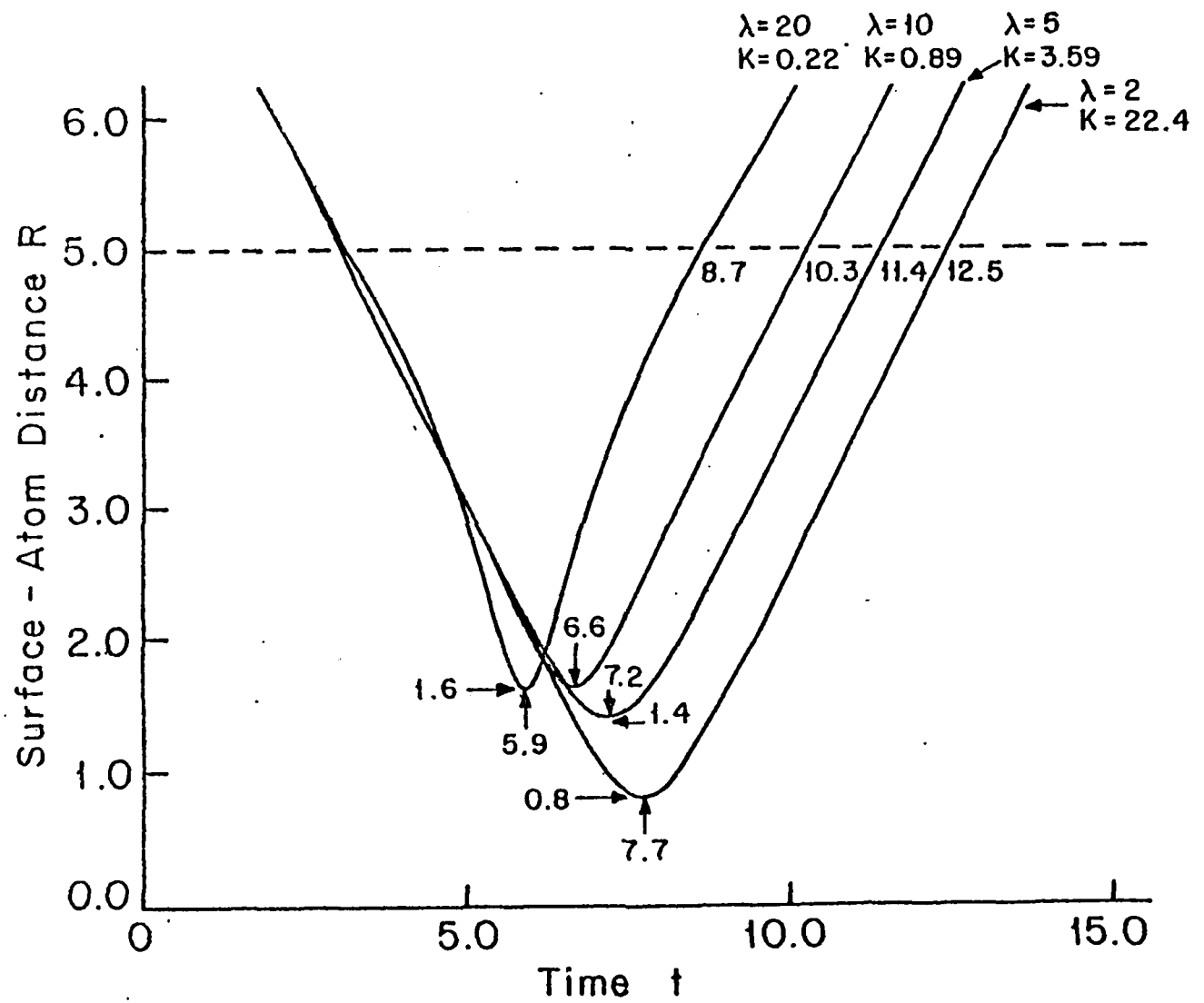
λ=20
K=0.22
λ=10
K=0.89
λ=5
K=3.59
λ=2
K=22.4
6.0
5.0
4.0
3.0
2.0
1.0
0.0
Surface - Atom Distance R
8.7
10.3
11.4
12.5
6.6
7.2
1.4
1.6
5.9
0.8
7.7
0
5.0
10.0
15.0
Time t

Fig 6

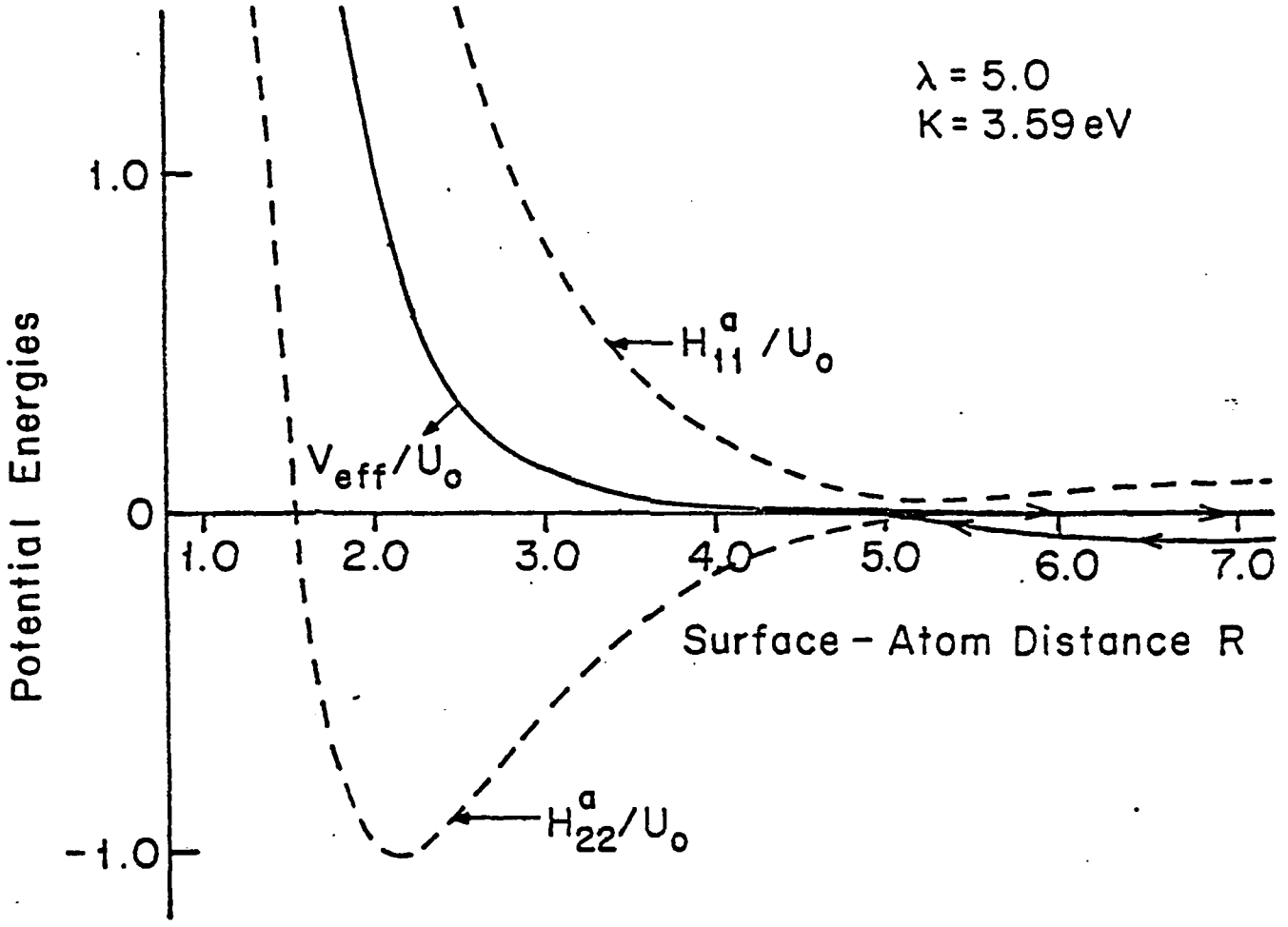
λ = 5.0
K = 3.59 eV
1.0
0
-1.0
Potential Energies
V_{eff}/U_o
H^a_{11}/U_o
H^a_{22}/U_o
1.0
2.0
3.0
4.0
5.0
6.0
7.0
Surface - Atom Distance R

Fig. 7

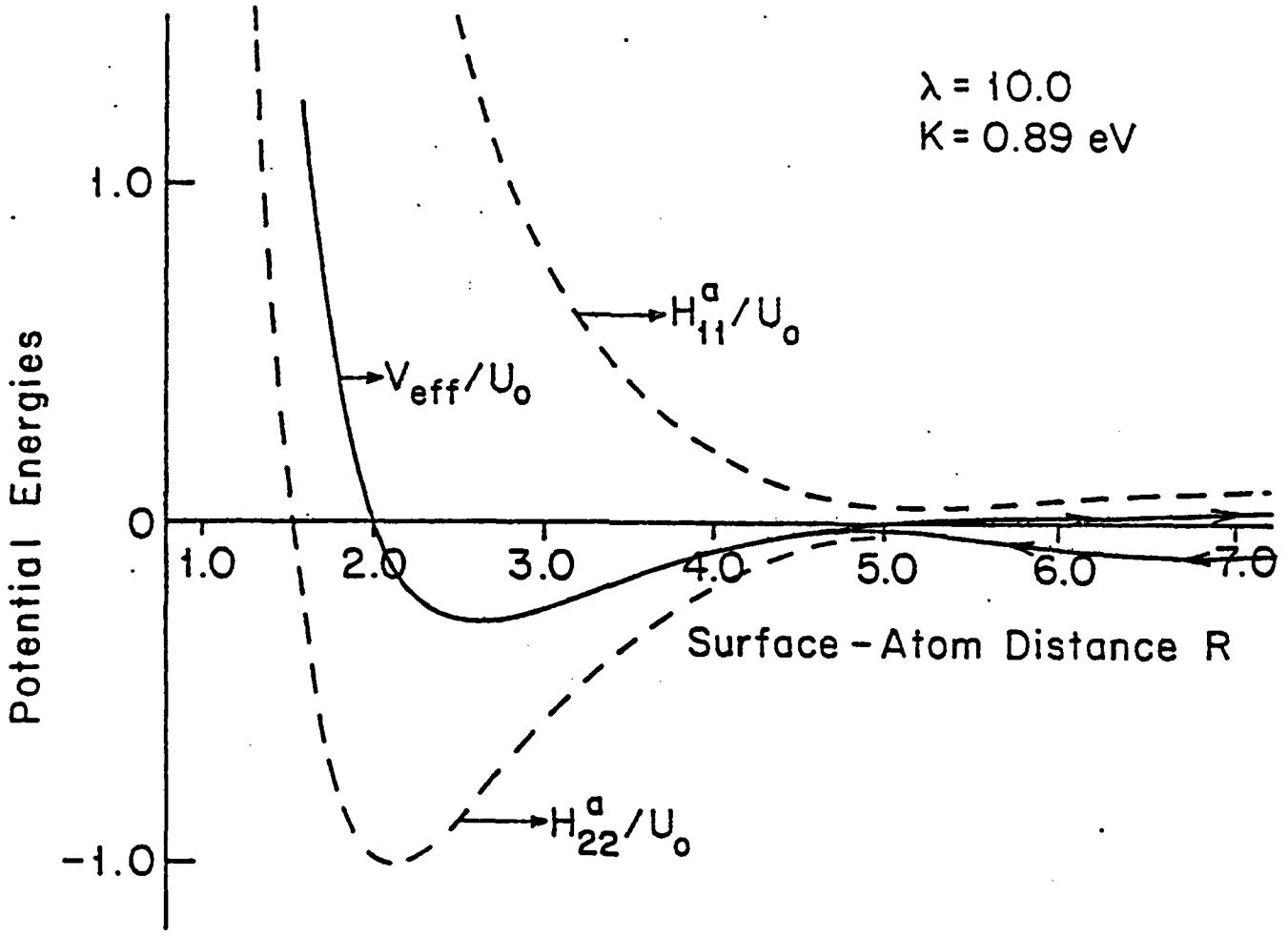
λ = 10.0
K = 0.89 eV
1.0
0
-1.0
Potential Energies
H^a_{11}/U_o
V_{eff}/U_o
H^a_{22}/U_o
1.0
2.0
3.0
4.0
5.0
6.0
7.0
Surface - Atom Distance R

Fig. 7c

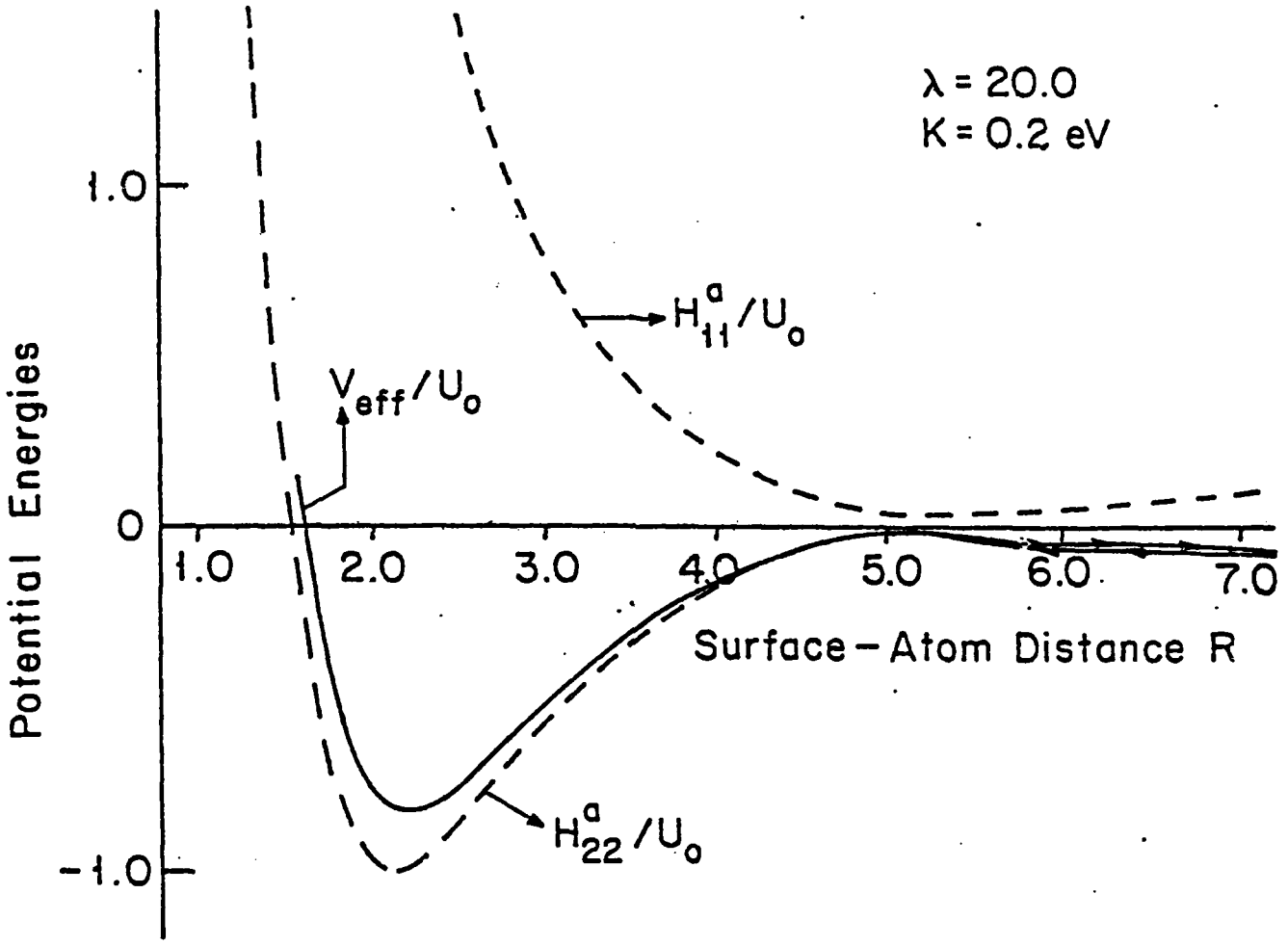
λ = 20.0
K = 0.2 eV
1.0
0
-1.0
Potential Energies
H^a_{11}/U_o
V_{eff}/U_o
H^a_{22}/U_o
1.0
2.0
3.0
4.0
5.0
6.0
7.0
Surface – Atom Distance R

Fig. 7d

Fig 8

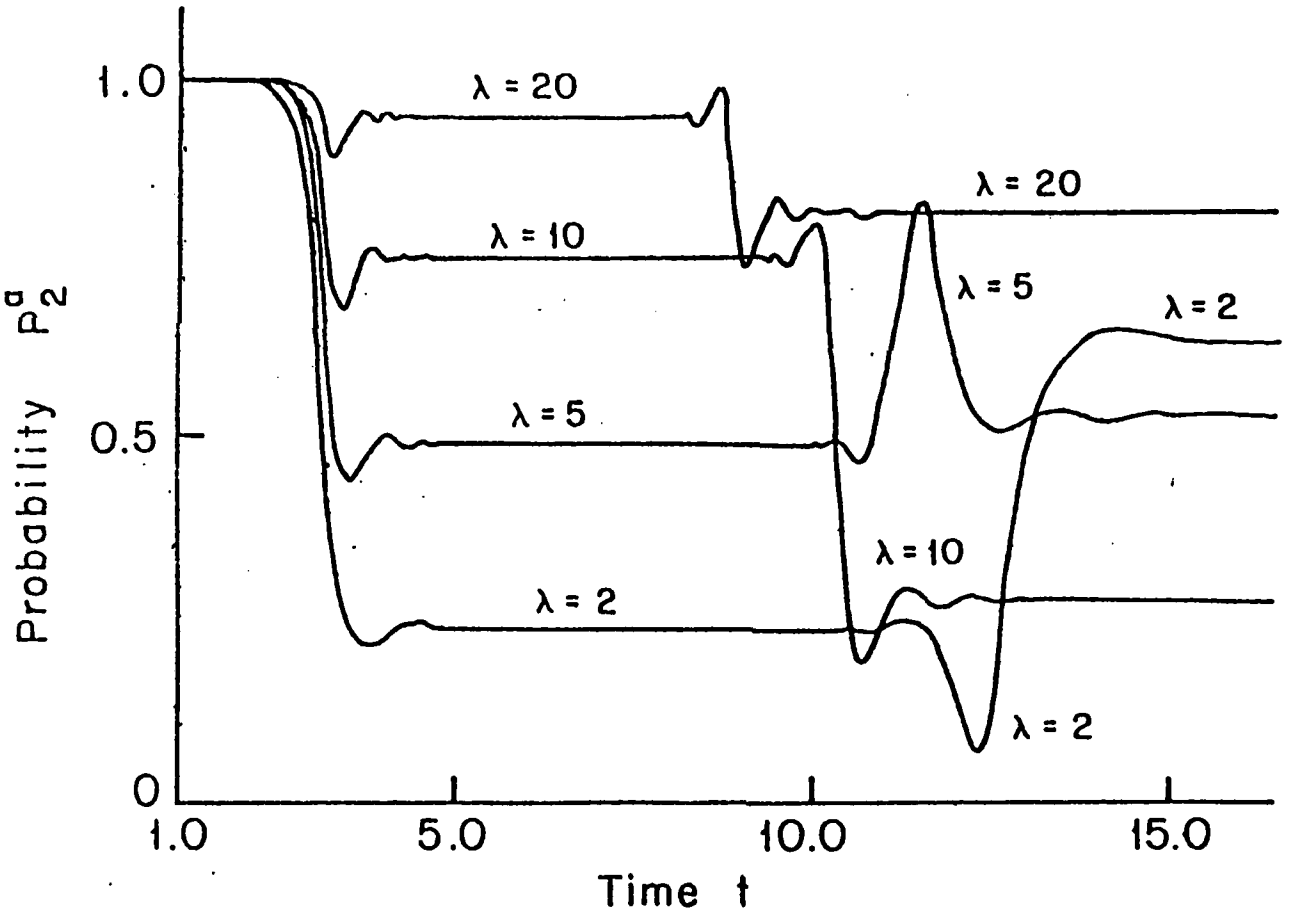
1.0
0.5
0
Probability P_2^a
λ = 20
λ = 10
λ = 5
λ = 2
λ = 20
λ = 5
λ = 2
λ = 10
λ = 2
1.0
5.0
10.0
15.0
Time t

Fig. 7a

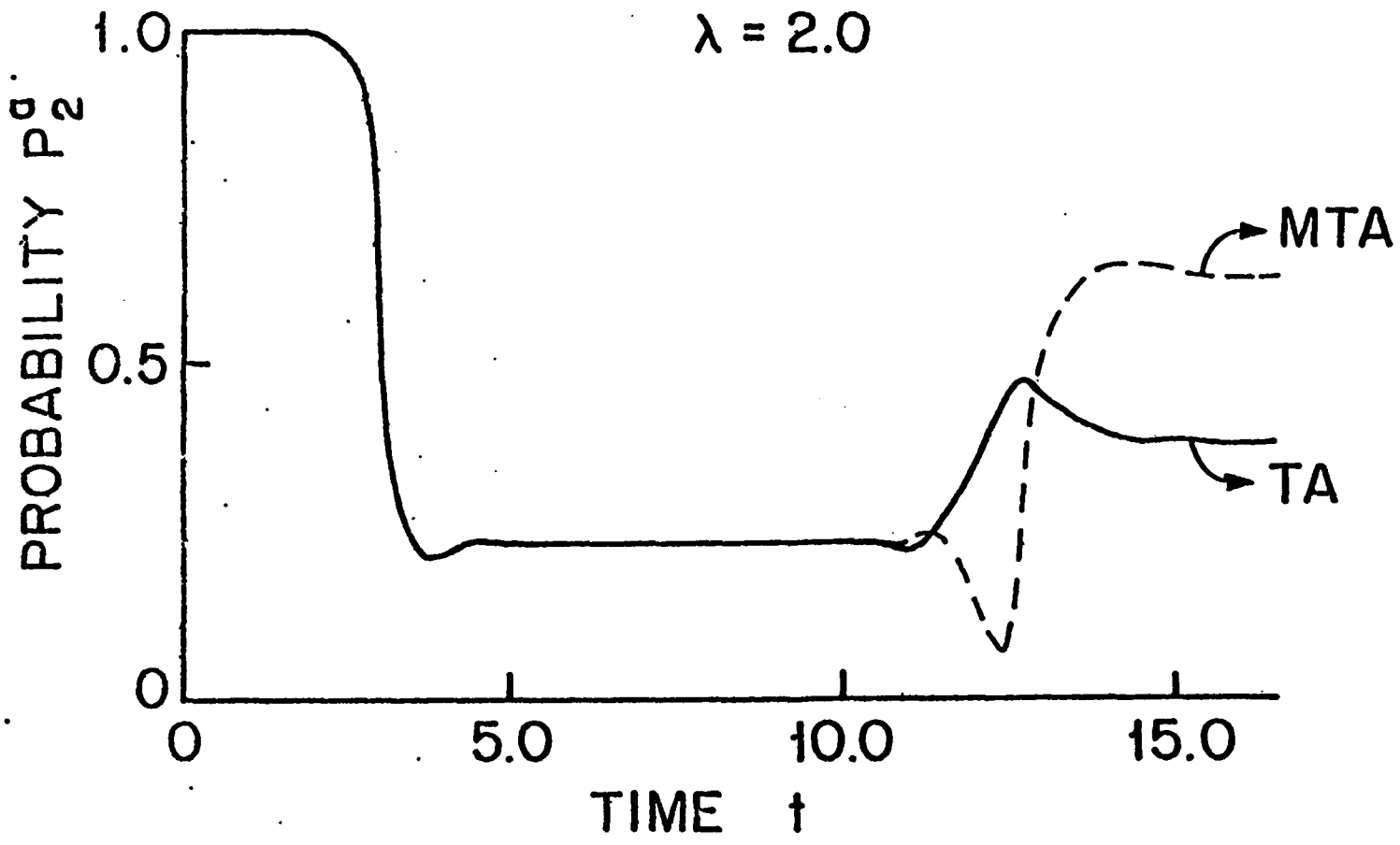

Fig 9b

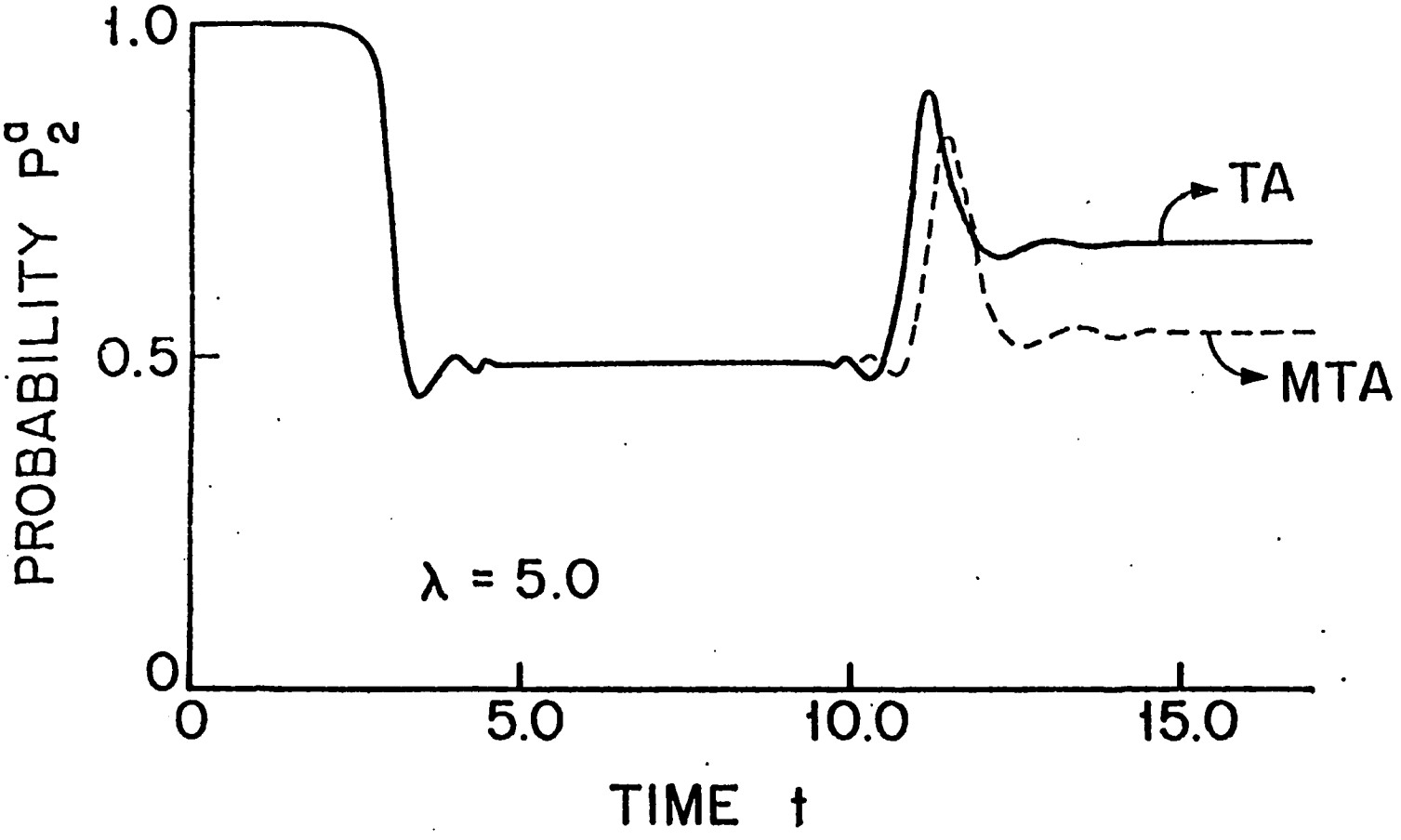

Fig 9.1

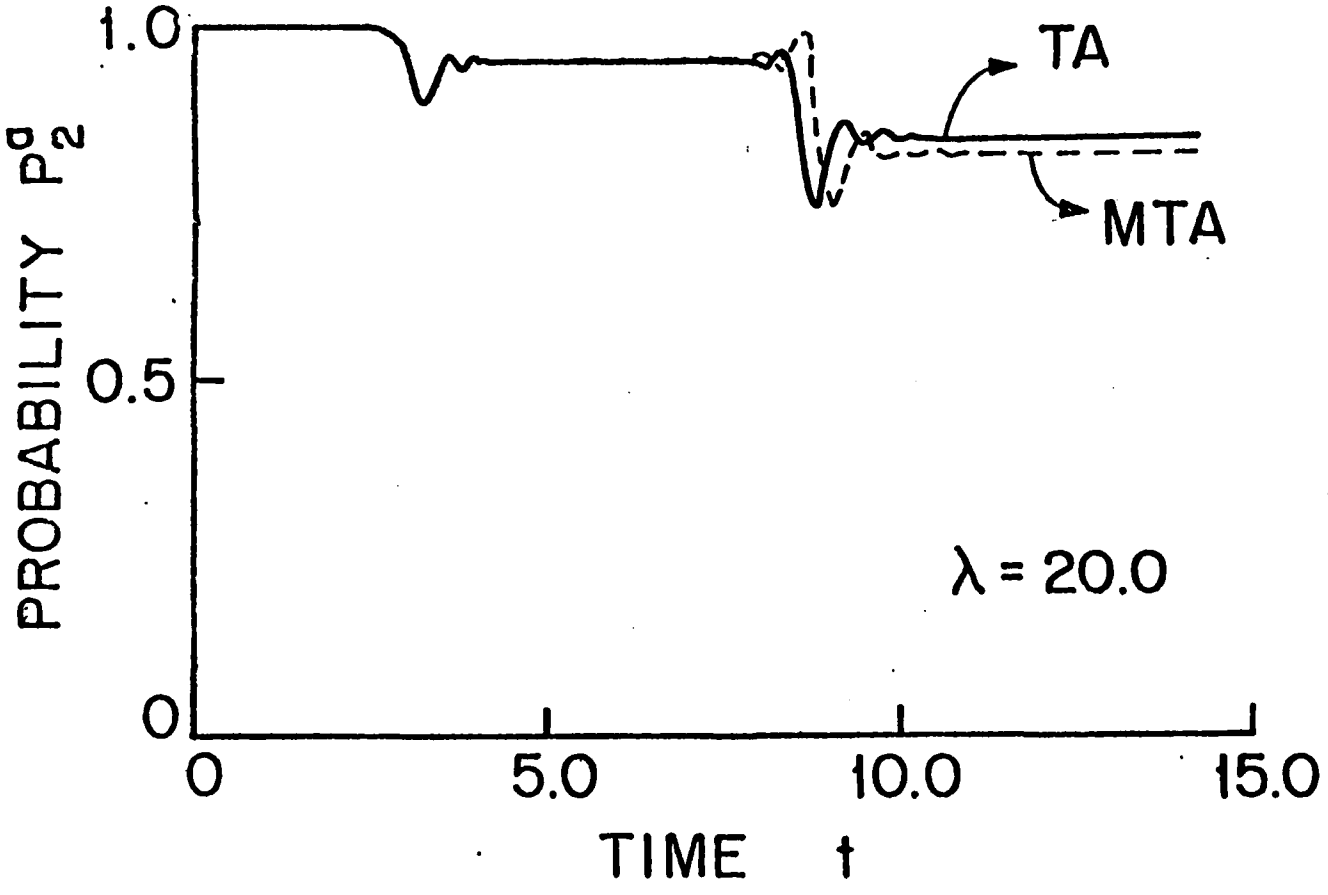

Fig. 7C

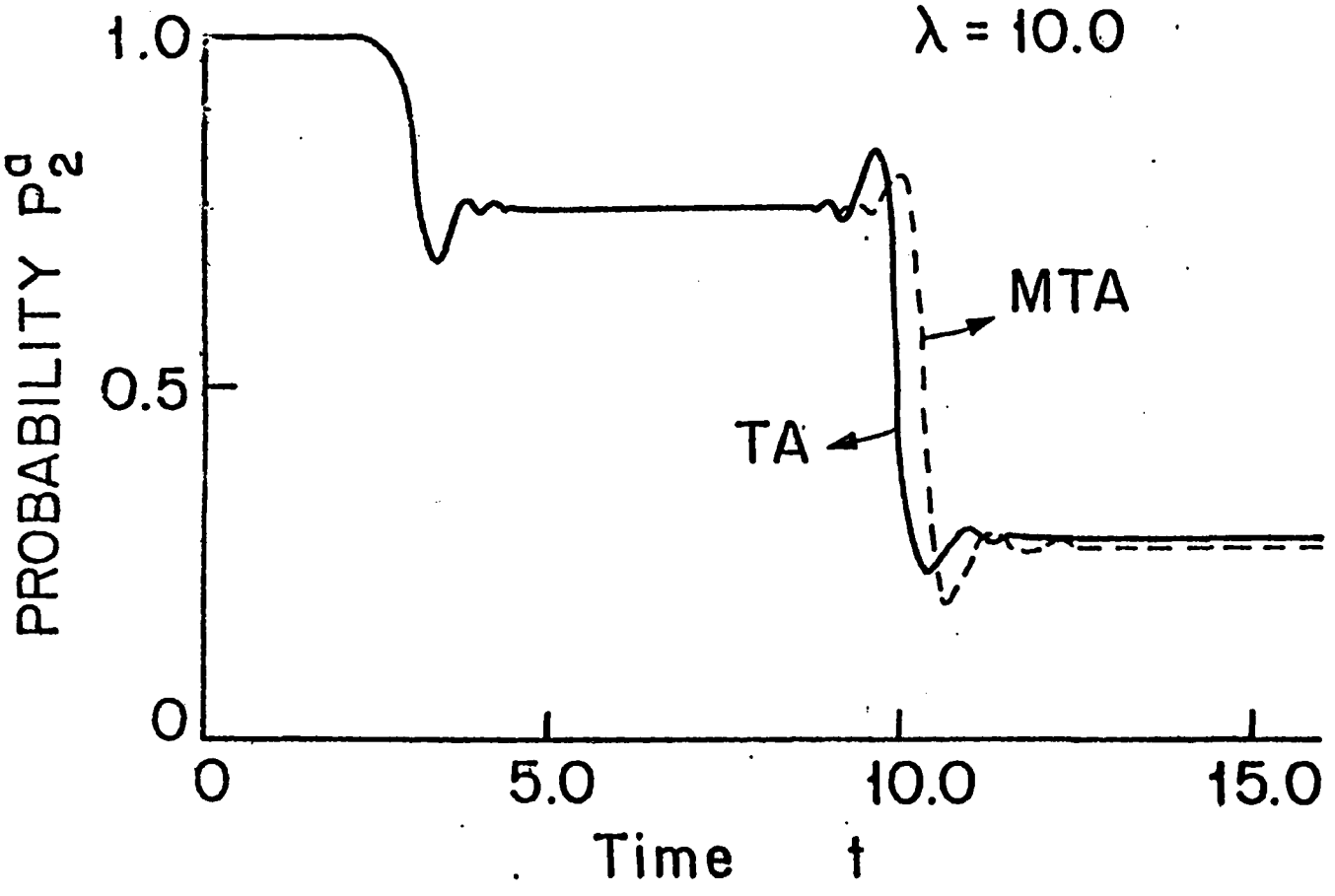

Fig 10

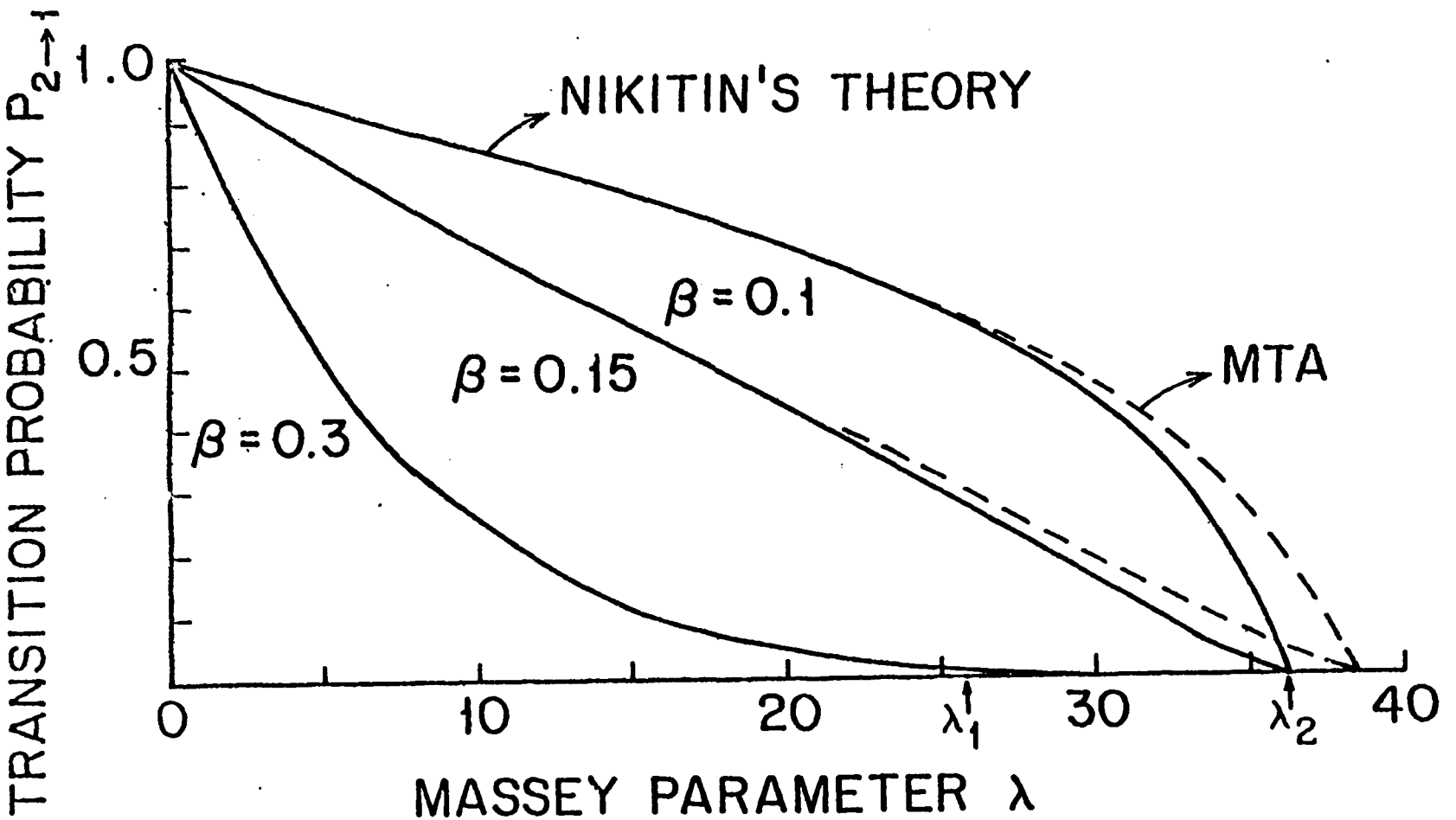
TRANSITION PROBABILITY $P_{2\to1}$
1.0
0.5
NIKITIN'S THEORY
$\beta = 0.1$
$\beta = 0.15$
$\beta = 0.3$
MTA
0
10
20
λ_1'
30
λ_2'
40
MASSEY PARAMETER λ

Fig. 11a

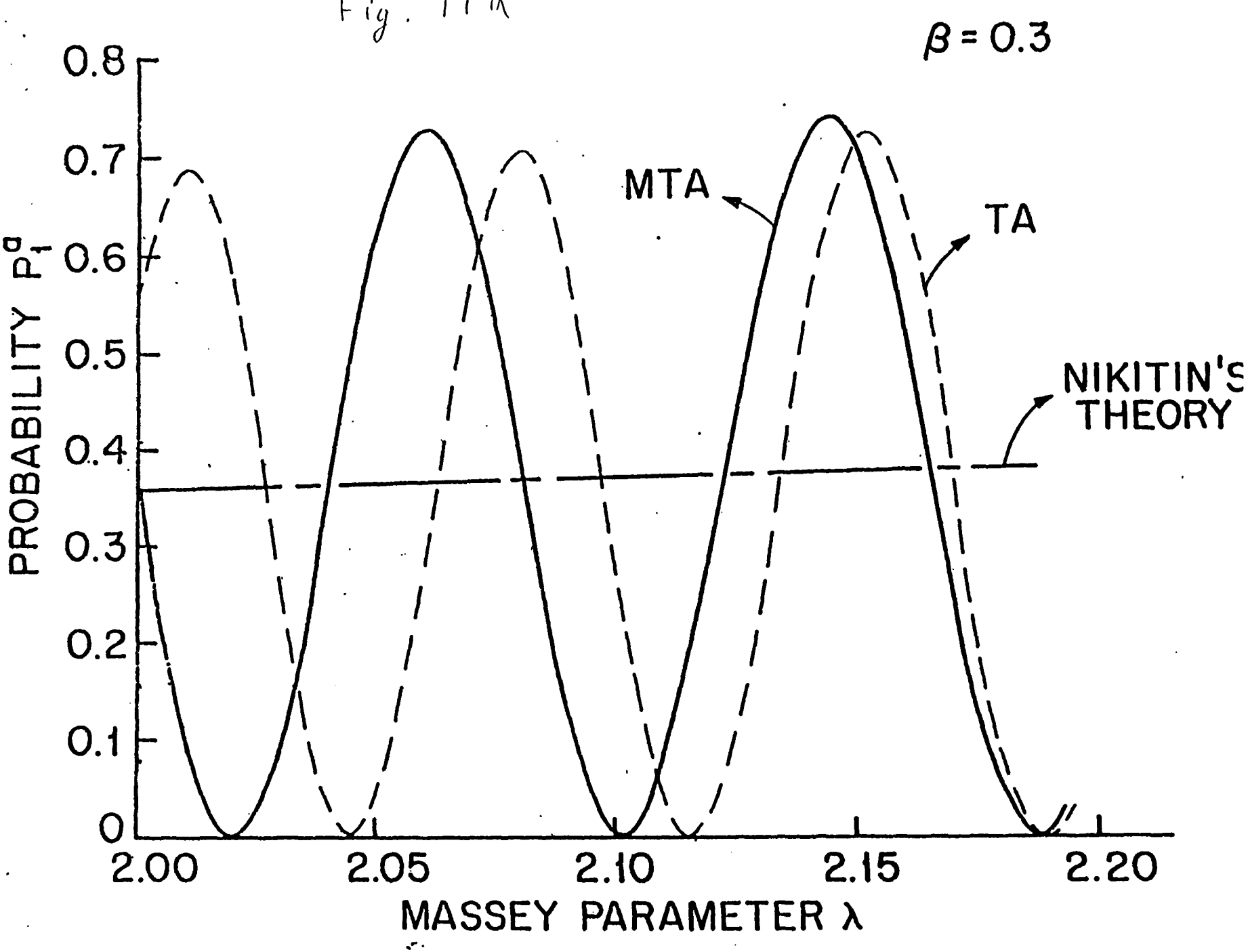
β = 0.3
MTA
TA
NIKITIN'S THEORY
PROBABILITY P_1^a
0.8
0.7
0.6
0.5
0.4
0.3
0.2
0.1
0
2.00
2.05
2.10
2.15
2.20
MASSEY PARAMETER λ

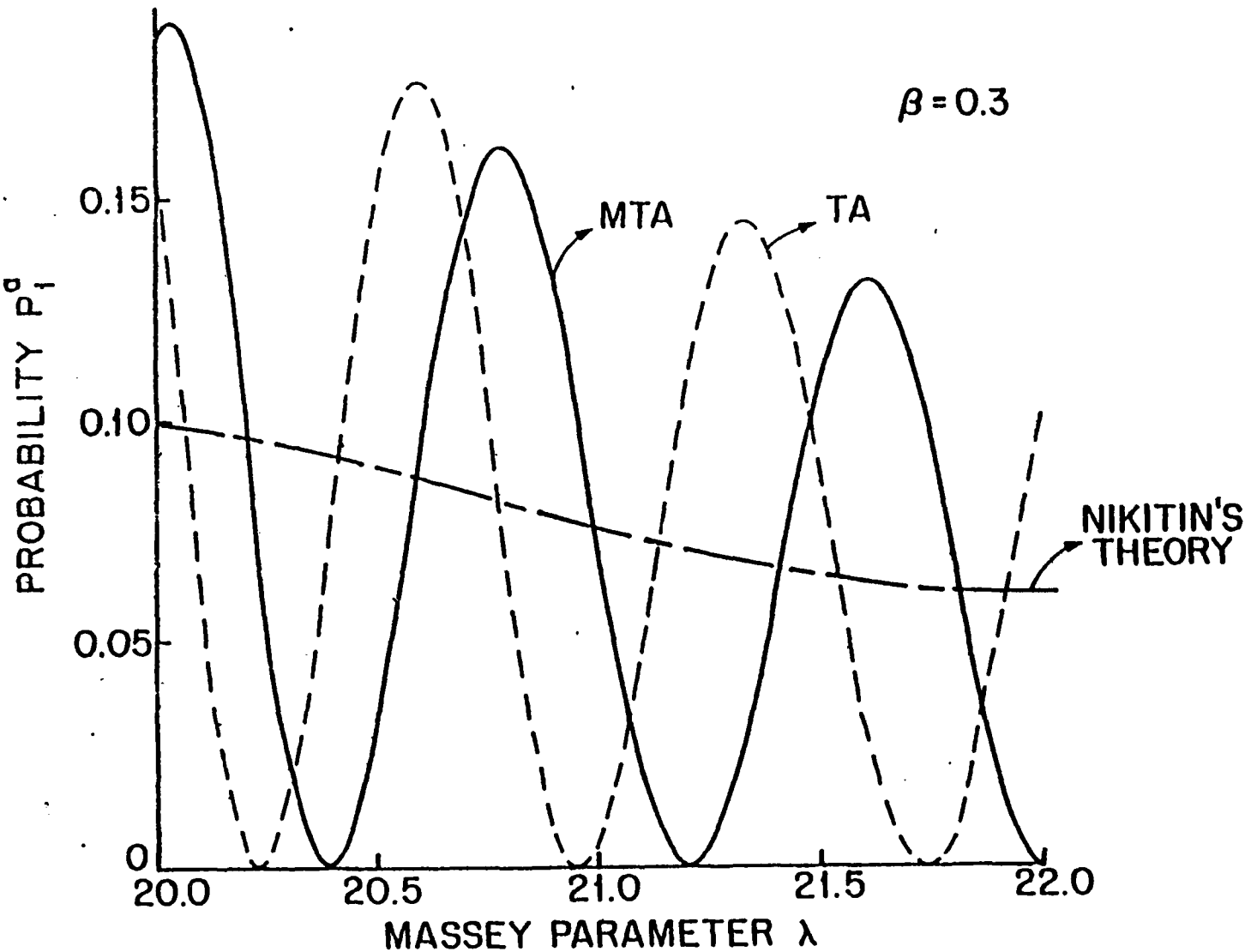
β = 0.3
MTA
TA
NIKITIN'S THEORY
PROBABILITY P_1^a
0.15
0.10
0.05
0
20.0
20.5
21.0
21.5
22.0
MASSEY PARAMETER λ

Fig 11 b

Fig 12a

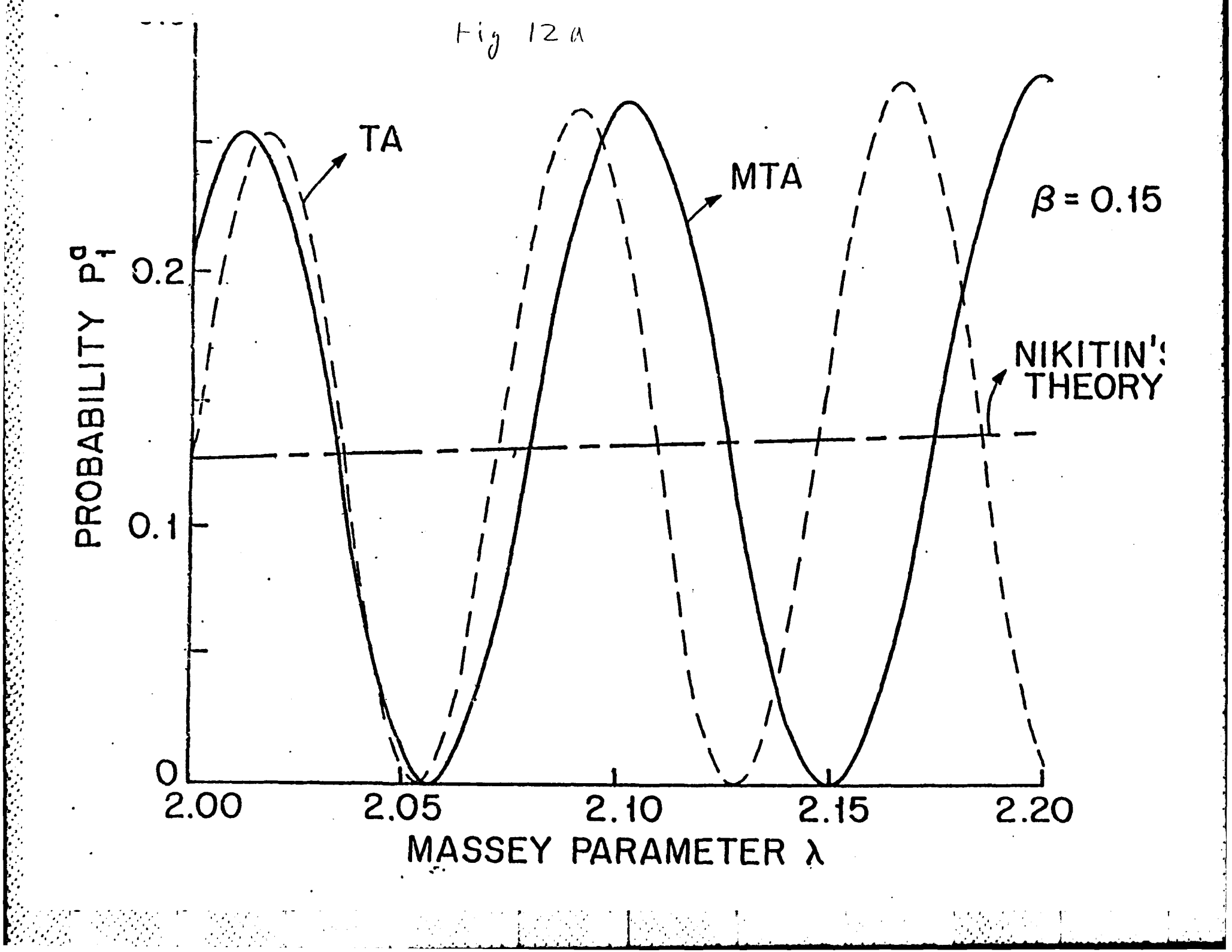
TA
MTA
β = 0.15
NIKITIN'S
THEORY
PROBABILITY P_1^a
0
0.1
0.2
2.00
2.05
2.10
2.15
2.20
MASSEY PARAMETER λ

Fig 12.b

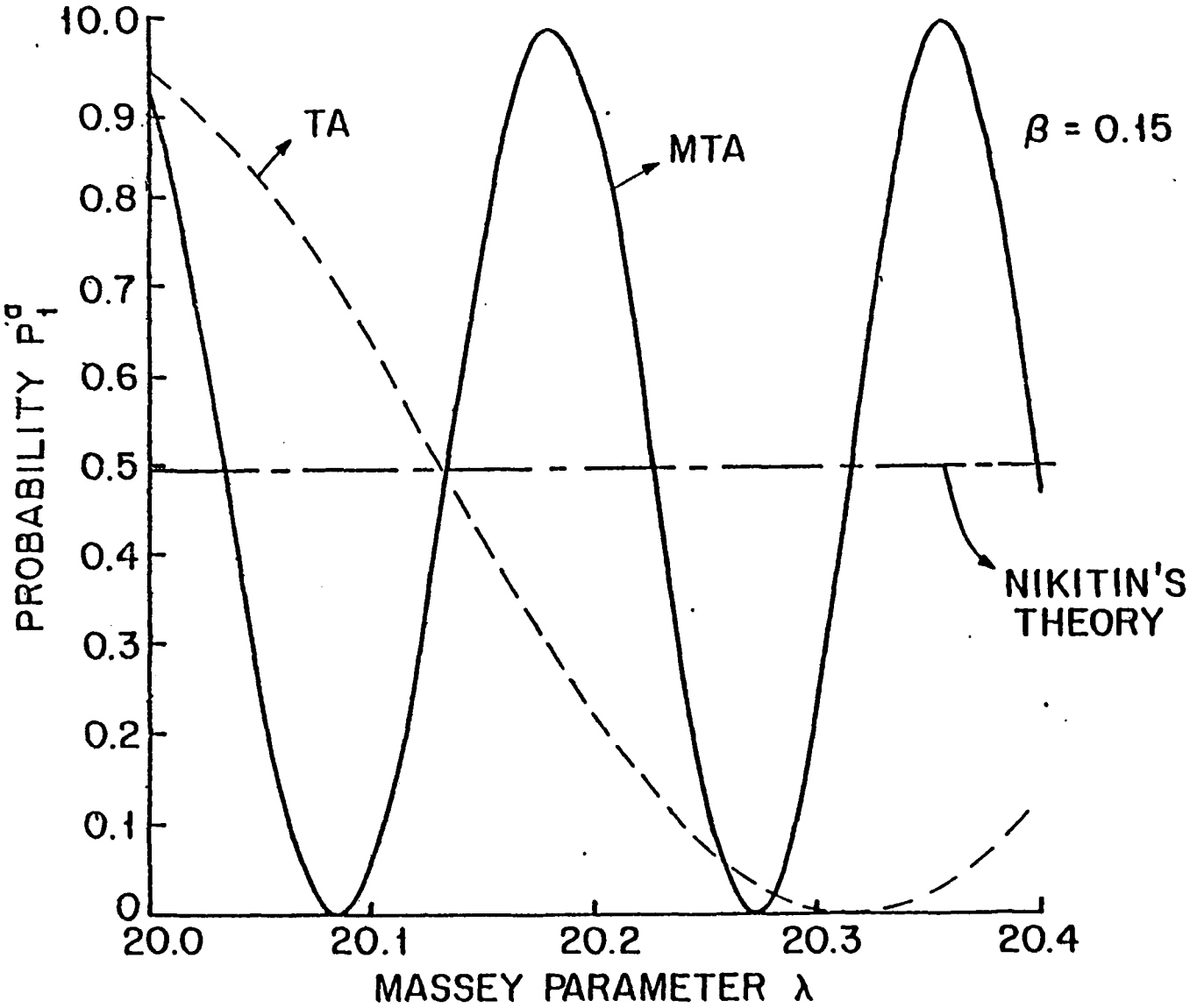
10.0
0.9
0.8
0.7
0.6
0.5
0.4
0.3
0.2
0.1
0
PROBABILITY P_1^a
TA
MTA
$\beta = 0.15$
NIKITIN'S THEORY
20.0
20.1
20.2
20.3
20.4
MASSEY PARAMETER λ

Fig. 12 (

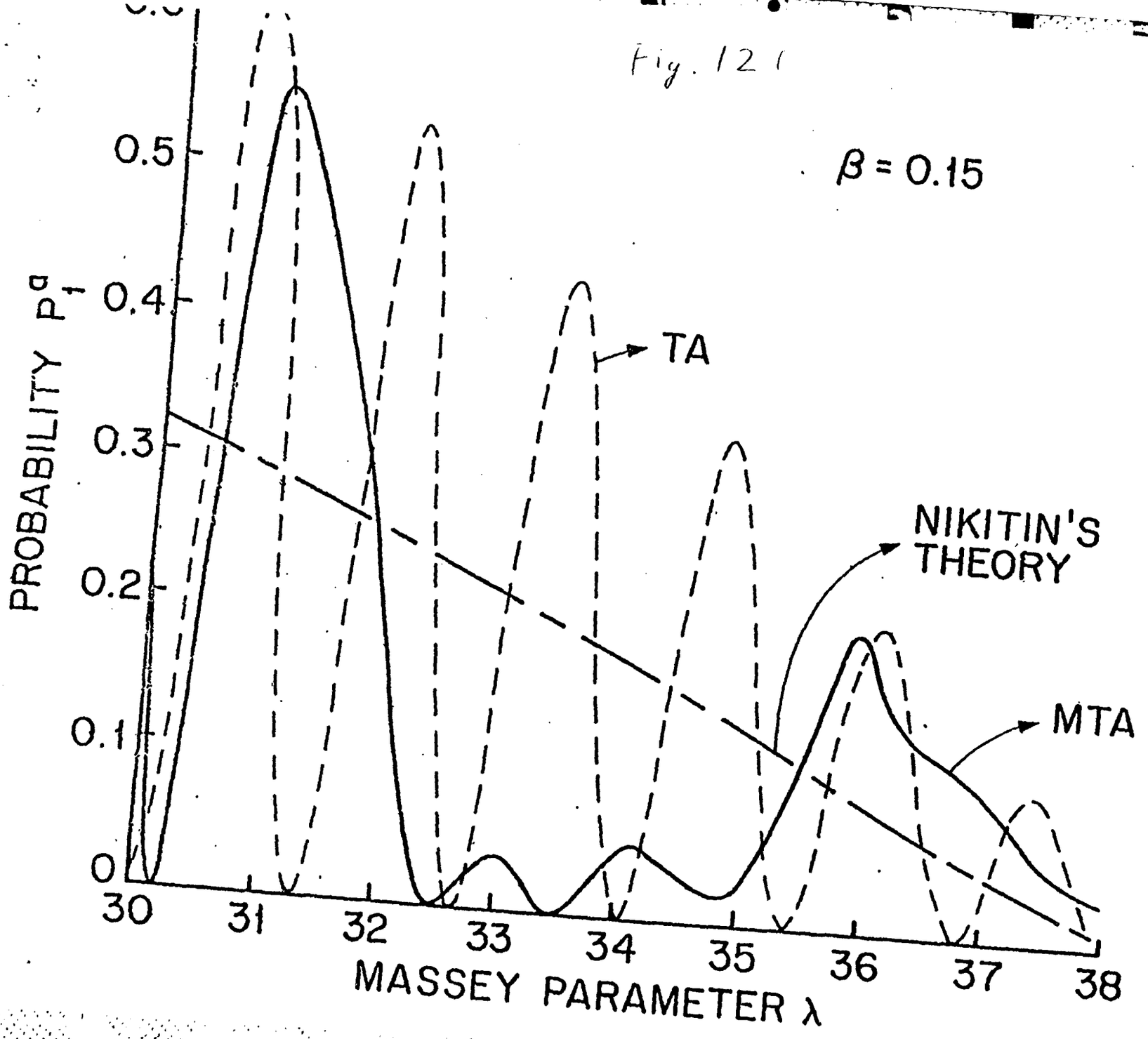
β = 0.15
TA
NIKITIN'S THEORY
MTA
PROBABILITY P_1^a
0.5
0.4
0.3
0.2
0.1
0
30
31
32
33
34
35
36
37
38
MASSEY PARAMETER λ

Fig 13

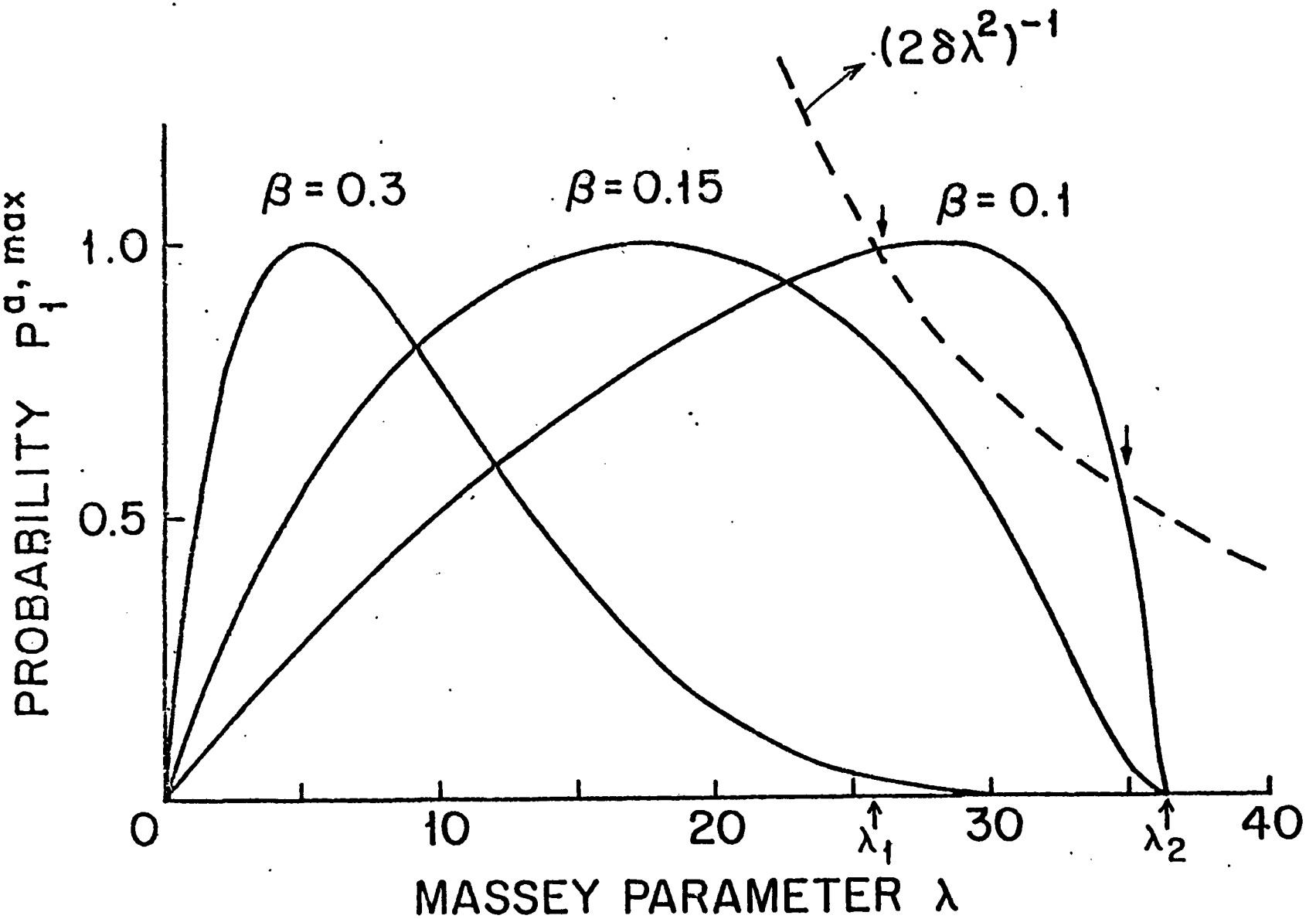
$(2\delta\lambda^2)^{-1}$
$\beta = 0.3$
$\beta = 0.15$
$\beta = 0.1$
PROBABILITY $P_1^{a,max}$
1.0
0.5
0
10
20
λ_1
30
λ_2
40
MASSEY PARAMETER λ

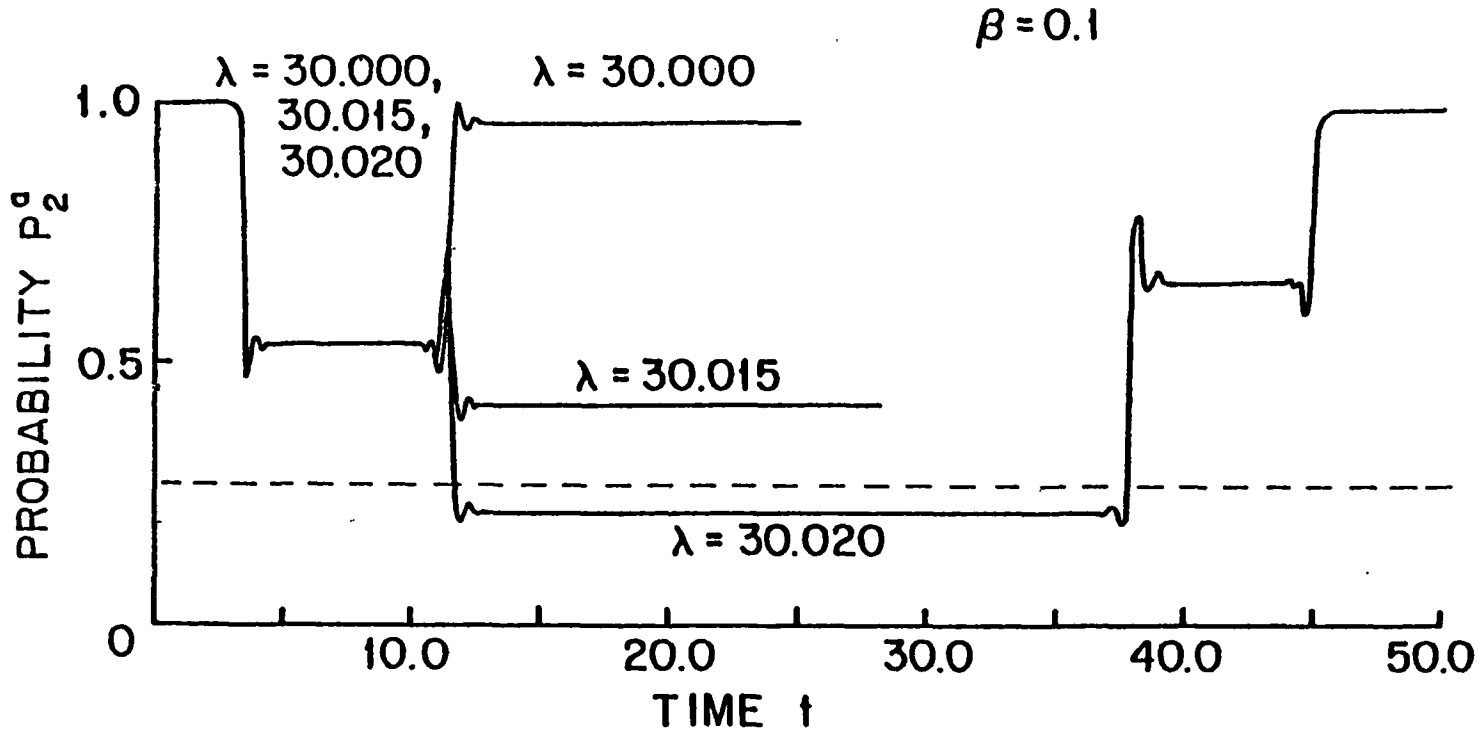
β = 0.1
λ = 30.000,
30.015,
30.020
λ = 30.000
λ = 30.015
λ = 30.020
1.0
0.5
0
PROBABILITY P_2^a
10.0
20.0
30.0
40.0
50.0
TIME t

Fig 14.a

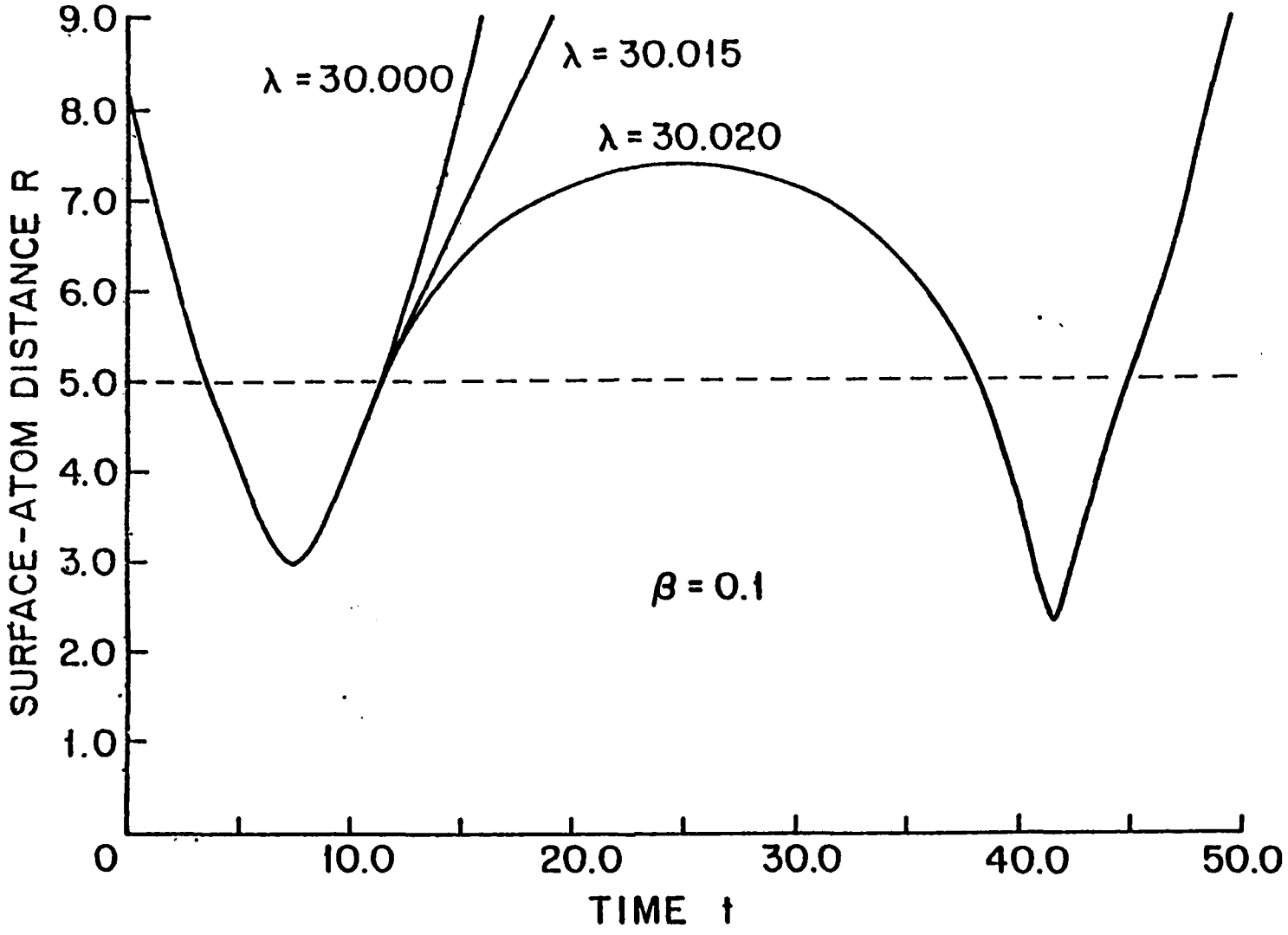
9.0
8.0
7.0
6.0
5.0
4.0
3.0
2.0
1.0
SURFACE-ATOM DISTANCE R
λ = 30.000
λ = 30.015
λ = 30.020
β = 0.1
0
10.0
20.0
30.0
40.0
50.0
TIME t

Fig 19. b

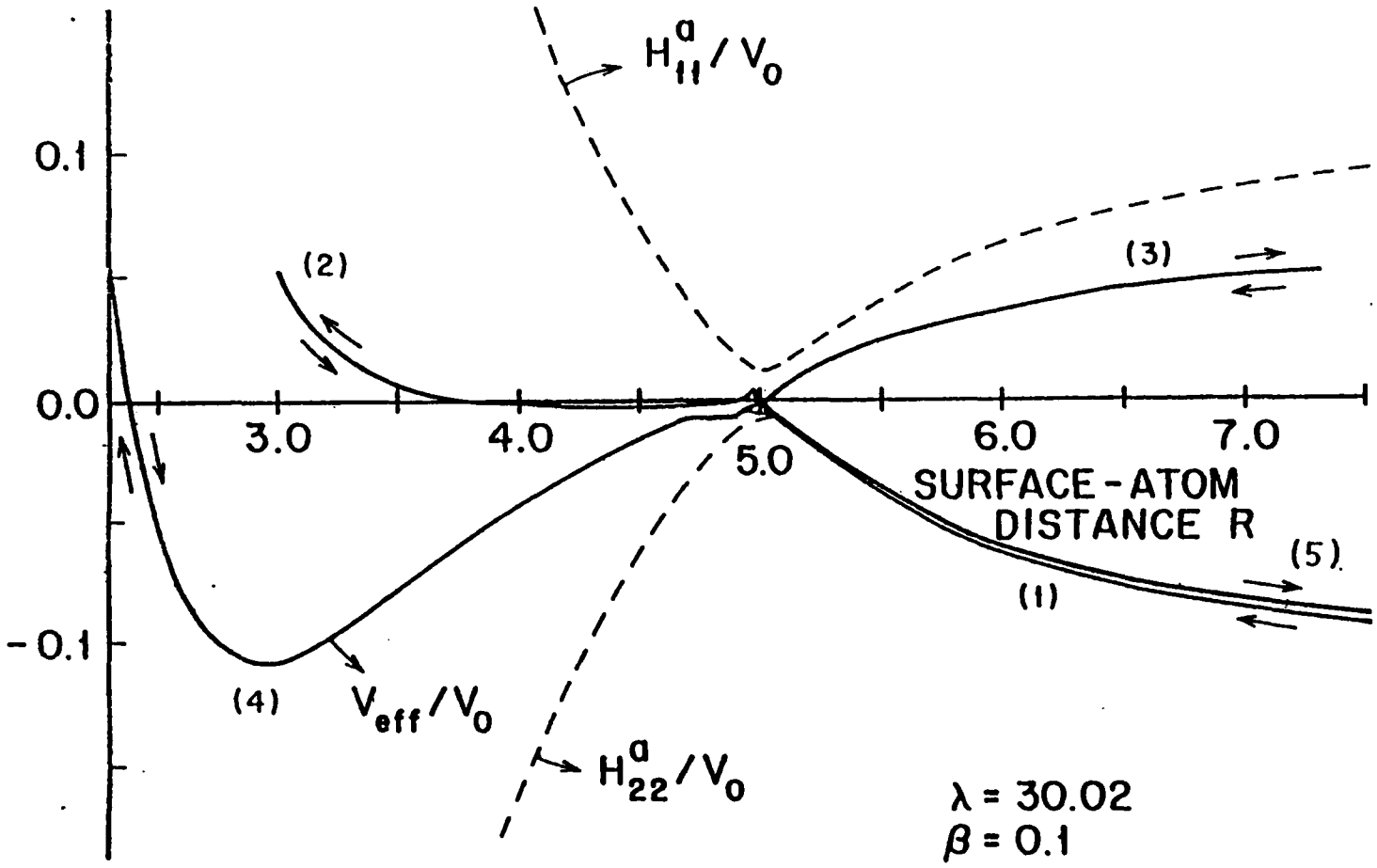
H^a_{11}/V_0
0.1
0.0
-0.1
(2)
(3)
3.0
4.0
5.0
6.0
7.0
SURFACE-ATOM
DISTANCE R
(5)
(1)
(4)
V_{eff}/V_0
H^a_{22}/V_0
$\lambda = 30.02$
$\beta = 0.1$

Fig 19.c

Fig 15a

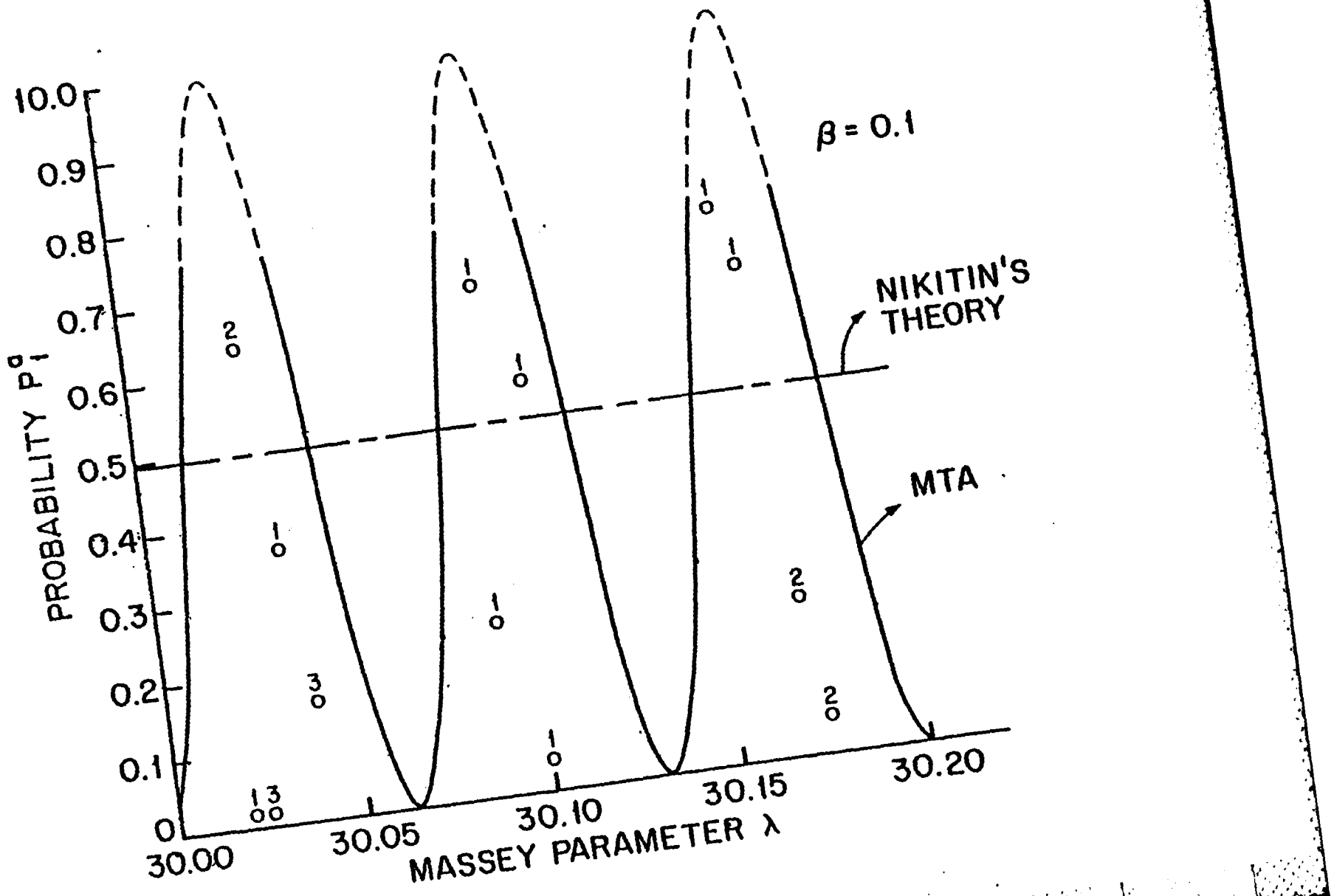
β = 0.1
NIKITIN'S THEORY
MTA
PROBABILITY P_1^0
MASSEY PARAMETER λ
10.0
0.9
0.8
0.7
0.6
0.5
0.4
0.3
0.2
0.1
0
30.00
30.05
30.10
30.15
30.20

Fig 15b

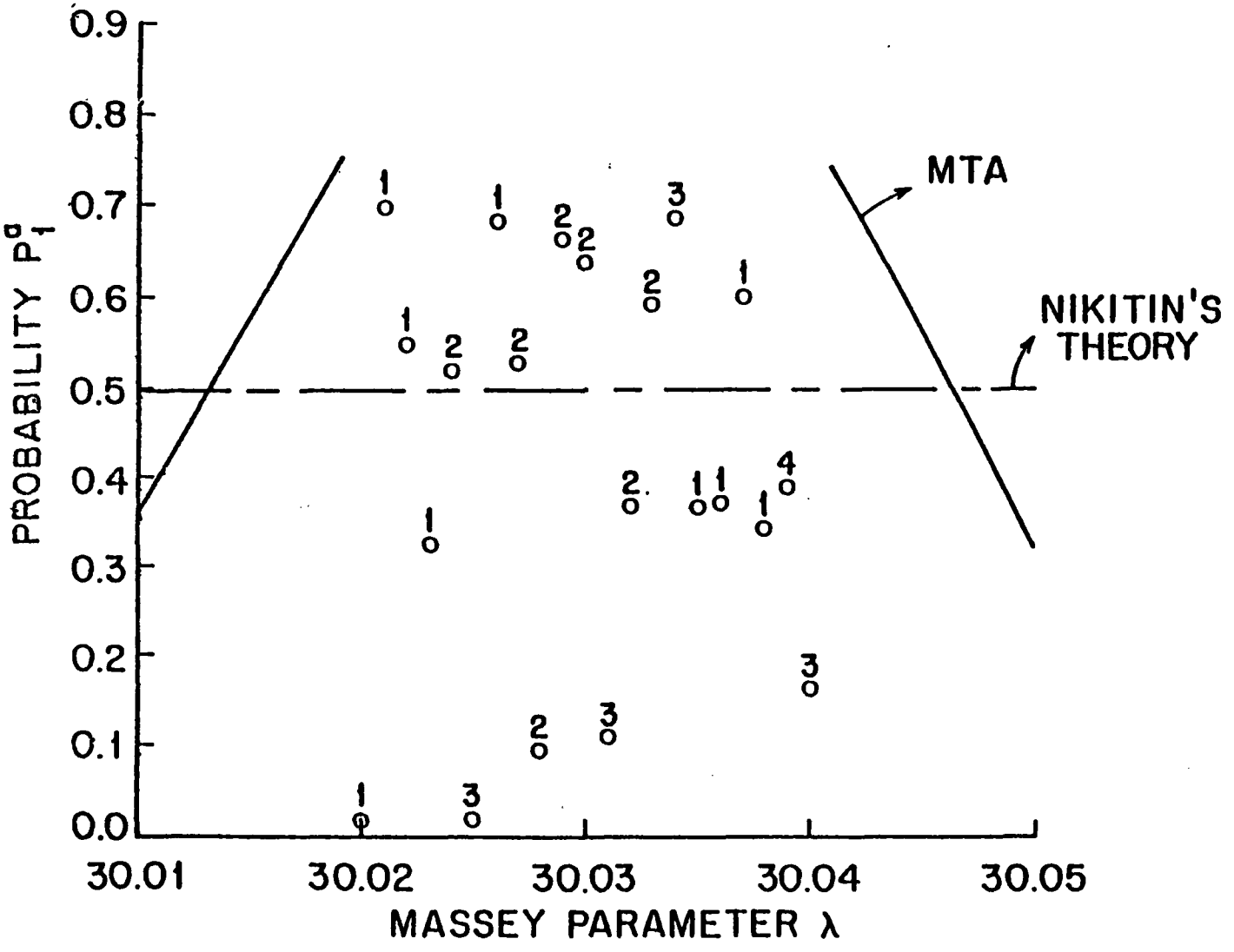
0.9
0.8
0.7
0.6
0.5
0.4
0.3
0.2
0.1
0.0
PROBABILITY P_1^a
MTA
NIKITIN'S THEORY
30.01
30.02
30.03
30.04
30.05
MASSEY PARAMETER λ

Fig 16 a.

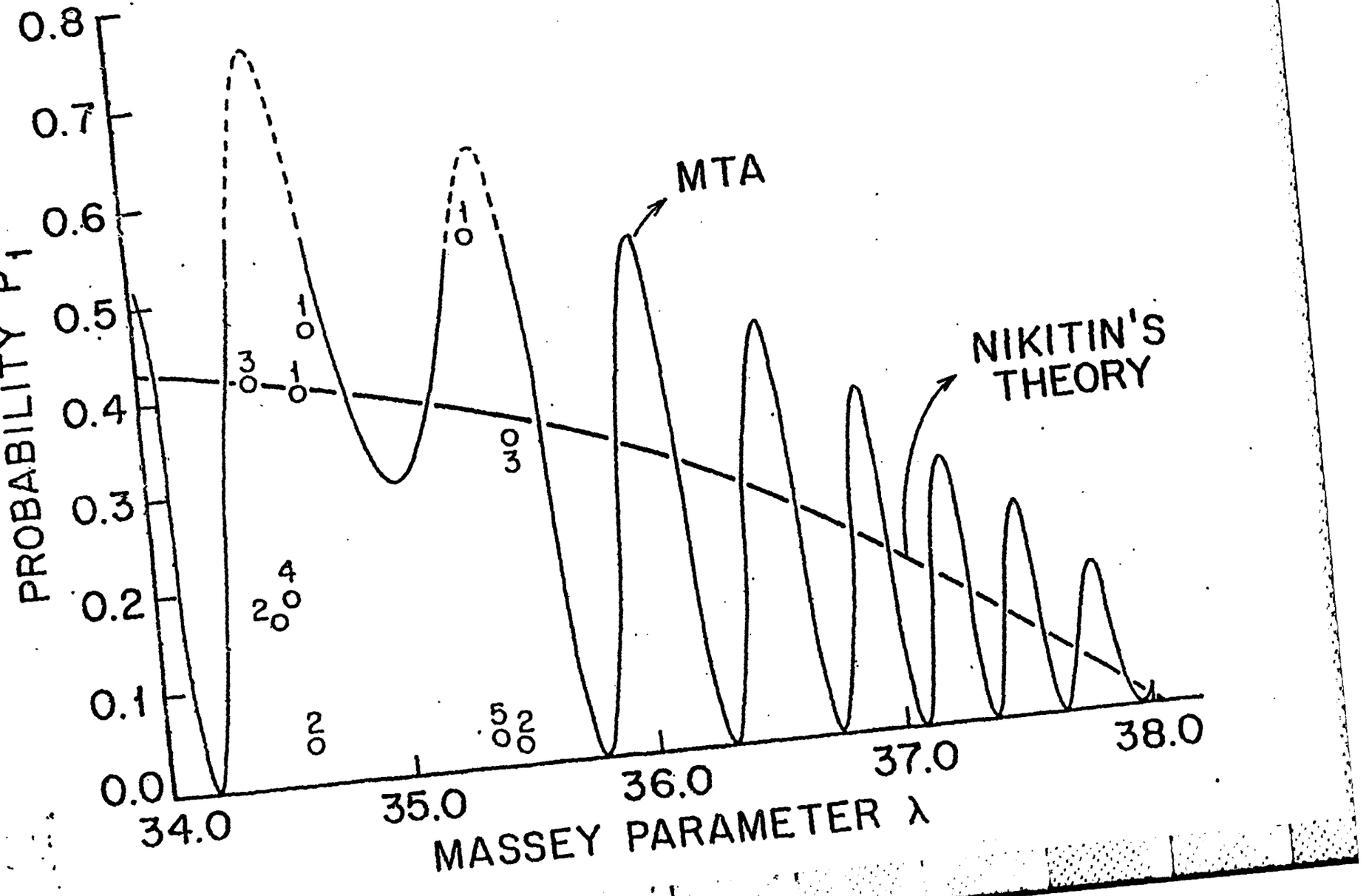
0.8
0.7
0.6
0.5
0.4
0.3
0.2
0.1
0.0
PROBABILITY P_1^a
34.0
35.0
36.0
37.0
38.0
MASSEY PARAMETER λ
MTA
NIKITIN'S THEORY
3 0
1 0
1 0
4 2 0
2 0
0 3
1 0
5 2 0

Fig 16. b

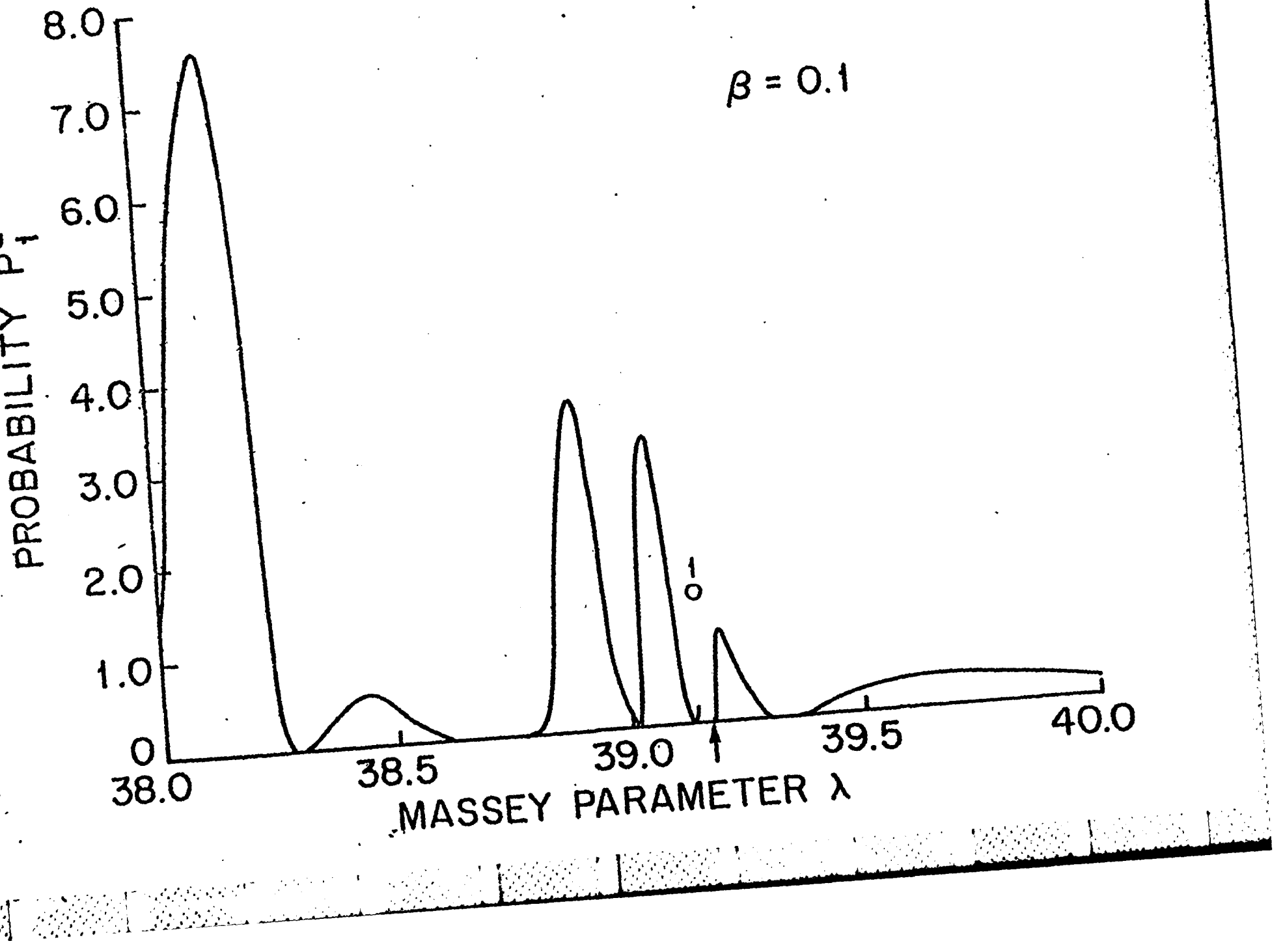
β = 0.1
8.0
7.0
6.0
5.0
4.0
3.0
2.0
1.0
0
PROBABILITY P_1^a
1
0
38.0
38.5
39.0
39.5
40.0
MASSEY PARAMETER λ

Fig 5.c

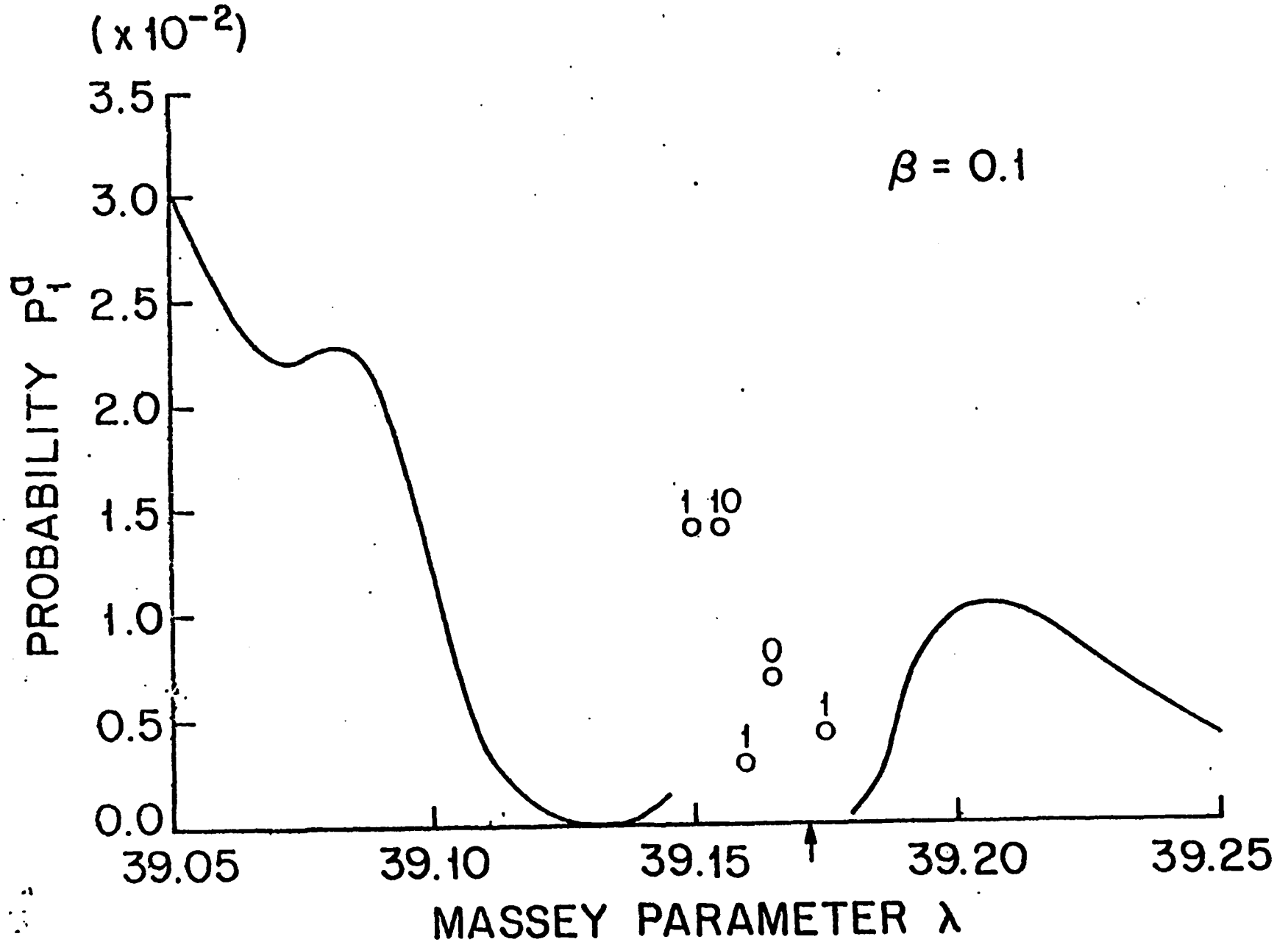
(x 10⁻²)
3.5
3.0
2.5
2.0
1.5
1.0
0.5
0.0
PROBABILITY P_1^a
β = 0.1
1 10
0
1
1
39.05
39.10
39.15
39.20
39.25
MASSEY PARAMETER λ

END

FILMED

5-85

DTIC